

Experimental Thermodynamics (30 common techniques)

Thermal analysis

Calorimetry

Differential Scanning Calorimetry

Modulated DSC

Microcalorimetry

Differential Thermal Analysis

Bomb Calorimetry/Combustion Calorimetry

Thermal Gravimetric Analysis/DTA/MS/IR/Raman

Colligative Analysis

Membrane Osmometry

Vapor Pressure Osmometry

Melting point/Boiling point

Density

Archimedes Method

Helium Pycnometry

Density Gradient Column

Dilatometry

Sound Velocity

Shock Compression

Abbe Refractometer

Ellipsometer

Surfaces

Gas Adsorption

Contact Angle

Zeta Potential

X-ray and Neutron Reflectivity

Phase Structure

Light, X-ray, Neutron Scattering

Osmotic Compressibility

OM, SEM, TEM, AFM

XRD, NPD

Chemical Methods

Calorimetry

Thermal analysis

Calorimetry

Differential Scanning Calorimetry

Modulated DSC

Microcalorimetry

Differential Thermal Analysis

Thermal Gravimetric Analysis

Bomb Calorimetry/Combustion Calorimetry

Calorimetry

dT/dQ is measured in the DTA

dQ/dT is measured in the DSC

How to build a scanning calorimeter

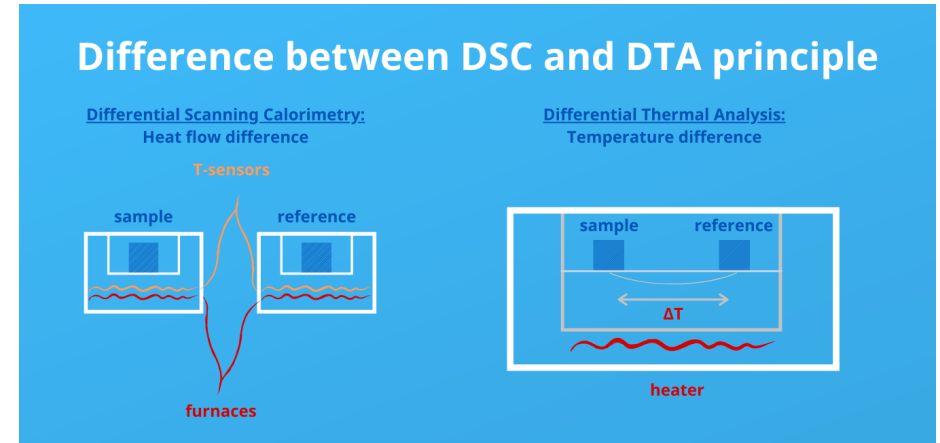
What is needed?

One or Two Adiabatic/Isolated Cells

Thermocouples, T

Heating rate, dQ/dt

Mass, m



Simplest approach and useful for very low or very high temperatures is **differential thermal analysis DTA**

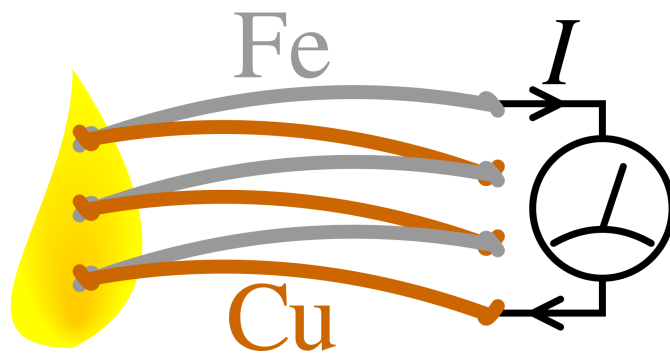
DTA is a simple design for difficult environments

Two cells heated at same rate and the difference in temperature is recorded

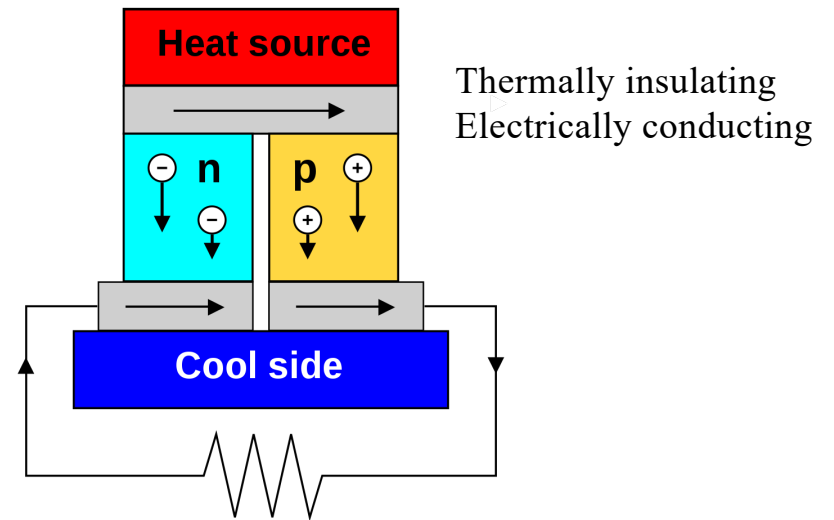
Differences in heat capacity and latent heats create differences in temperatures through transitions.

Measure the Temperature Seebeck Effect: Thermocouple

Electrons (or holes) flow from the hot side where they have high kinetic energy to the cold side where they have less kinetic energy. They will spend more time in the cold side, something like condensing in the cold side. This effect is different in magnitude for different metals or semiconductors. The difference in potential at the cold side between two metals is proportional to the temperature. (Similar to thermophoretic sampling.)



Thermocouple



Thermoelectric generator

Absolute calibration of the latent heat of transition using differential thermal analysis

Cite as: Rev. Sci. Instrum. 92, 075106 (2021); doi: 10.1063/5.0056857

Submitted: 14 May 2021 • Accepted: 1 July 2021 •

Published Online: 16 July 2021



View Online



Export Citation



CrossMark

Tapas Bar^{a)}  and Bhavtosh Bansal^{b)} 

AFFILIATIONS

Indian Institute of Science Education and Research Kolkata, Mohanpur Campus, Nadia 741246, West Bengal, India

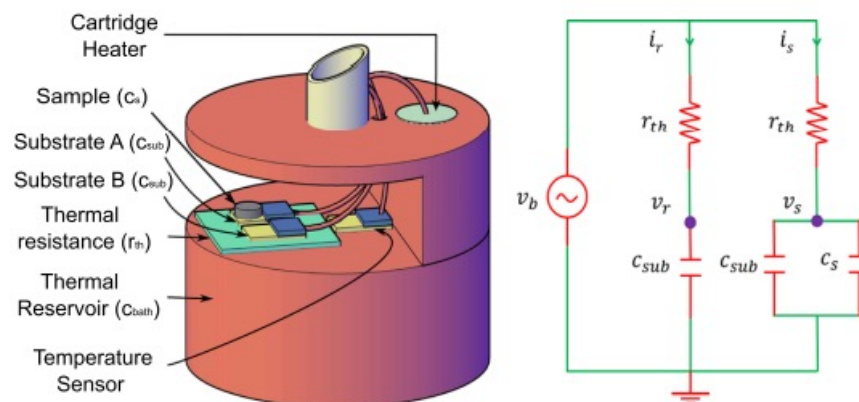


FIG. 1. (Left) Schematic of the calorimeter. The sample is mounted on substrate A, and the other nearly identical Pt-100 (substrate B) serves as the reference. An external temperature controller controls the temperature of the thermal reservoir through a temperature sensor and a cartridge heater, which is placed inside the thermal bath. (Right) Equivalent electrical circuit of the calorimeter based on analogy between Biot–Fourier and Ohm’s law.

Cryostat
Use liquid He or a
He refrigerator
4.2K boiling point



Calorimetry

$$dQ/dt = C_p dT/dt + \Delta H_{\text{transitions}}$$

$$\Delta Q = C_p (T_f - T_i) + \Delta H_{\text{transitions}}$$

$$T_f = T_i + (\Delta Q - \Delta H_{\text{transitions}})/C_p$$

$$\Delta Q = (dQ/dt) t$$

dT/dQ is measured in the DTA

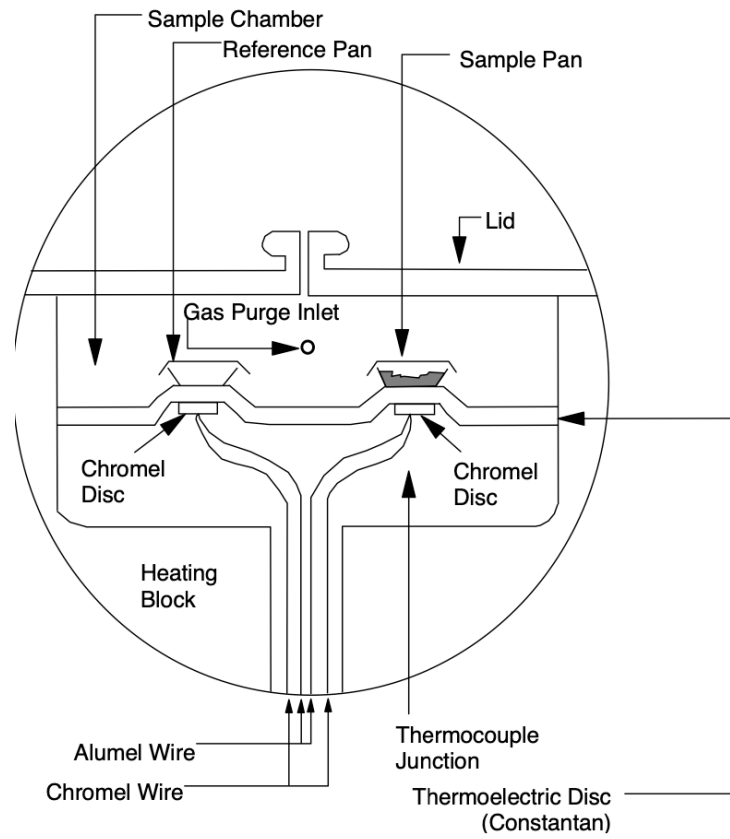
$$dQ/dt = (dT/dt)/(dT/dQ)$$

dQ/dT is measured in the DSC

$$dQ/dt = (dQ/dT) (dT/dt)$$

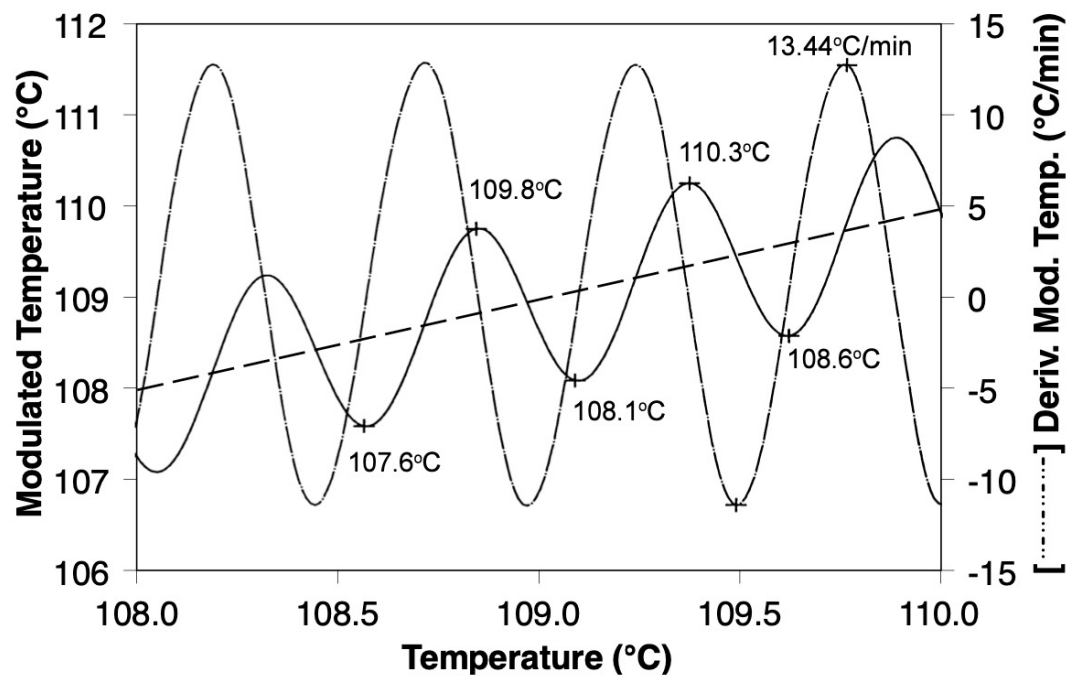
Modulated DSC

Figure 1: HEAT FLUX DSC SCHEMATIC



$$\frac{dT}{dt} = \beta + A_T \omega \cos(\omega t)$$

Figure 2: MDSC HEATING PROFILE



In the example shown in Figure 2, the underlying heating rate is 1°C/minute, the modulation period is 30 seconds, and the modulation amplitude is ±1°C. This set of conditions results in a sinusoidal heating profile where the instantaneous heating rate varies between +13.44°C/minute and -11.54°C/minute (i.e., cooling occurs during a portion of the modulation). Although the actual sample temperature changes in a sinusoidal fashion during this process (Figure 3), the analyzed signals are ultimately plotted versus the linear average temperature which is calculated from the average value as measured by the sample thermocouple (essentially the dashed line in Figure 2). [Note: As in conventional DSC, MDSC can also be run in a cooling rather than heating mode.]

$$\frac{dT}{dt} = \beta + A_T \omega \cos(\omega t)$$

$$\frac{dQ}{dt} = C_p \beta + f(T,t)$$

where: $\frac{dQ}{dt}$ = total heat flow

C_p = heat capacity

β = heating rate

$f(T,t)$ = heat flow from kinetic (absolute temperature and time dependent) processes

Figure 2: MDSC HEATING PROFILE



[1]

In the example shown in Figure 2, the underlying heating rate is 1°C/minute, the modulation period is 30 seconds, and the modulation amplitude is ±1°C. This set of conditions results in a sinusoidal heating profile where the instantaneous heating rate varies between +13.44°C/minute and -11.54°C/minute (i.e., cooling occurs during a portion of the modulation). Although the actual sample temperature changes in a sinusoidal fashion during this process (Figure 3), the analyzed signals are ultimately plotted versus the linear average temperature which is calculated from the average value as measured by the sample thermocouple (essentially the dashed line in Figure 2). [Note: As in conventional DSC, MDSC can also be run in a cooling rather than heating mode.]

Figure 7: MDSC RAW SIGNALS

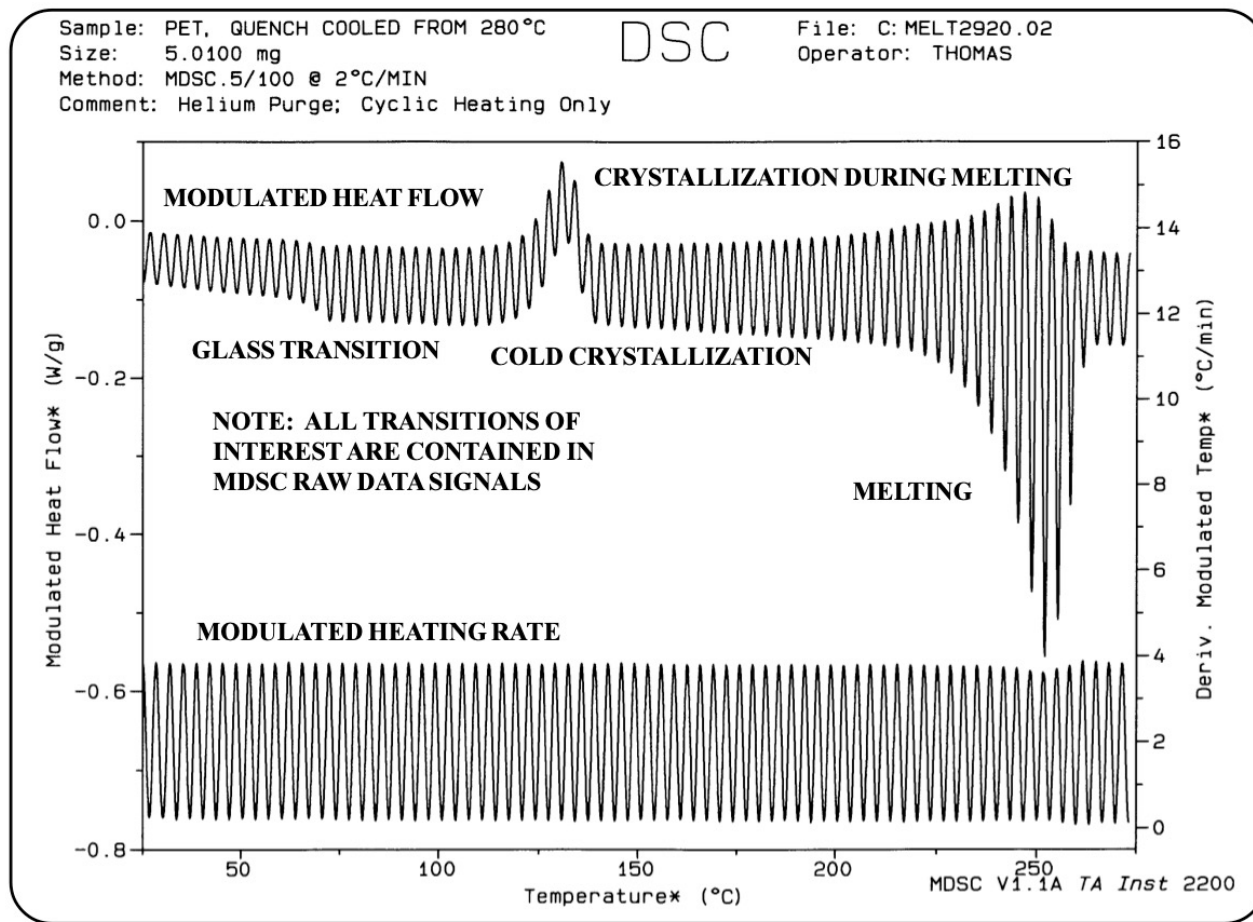


Figure 8: DSC Cp MEASUREMENT

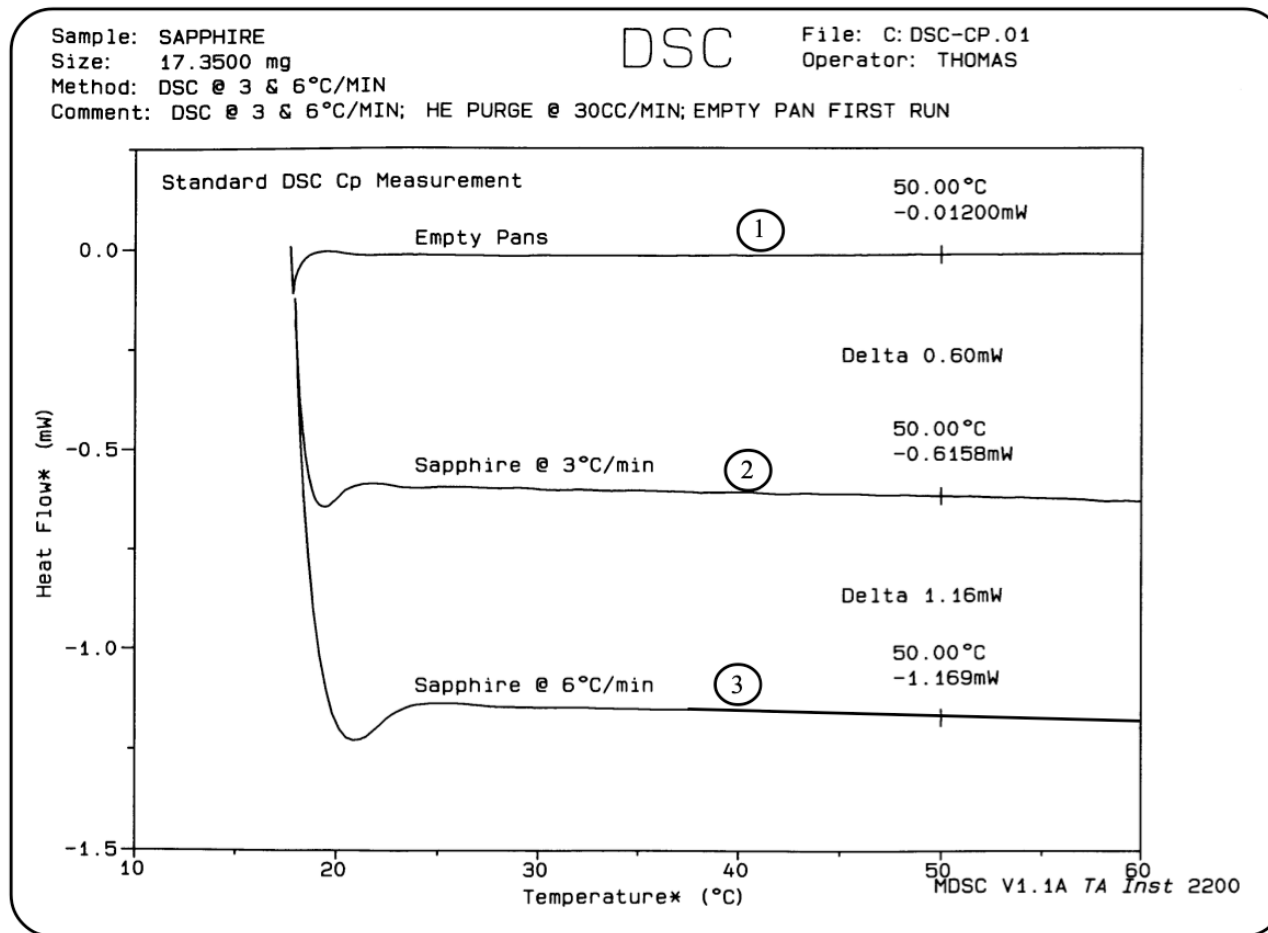


Figure 9: MDSC Cp MEASUREMENT

Sample: SAPPHIRE
Size: 17.3500 mg
Method: MDSC .4/100 @ 4.5°C/MIN
Comment: DSC .4/100 @ 4.5°C/MIN; HE PURGE @ 30CC/MIN

DSC

File: C: DSC-CP.02
Operator: THOMAS

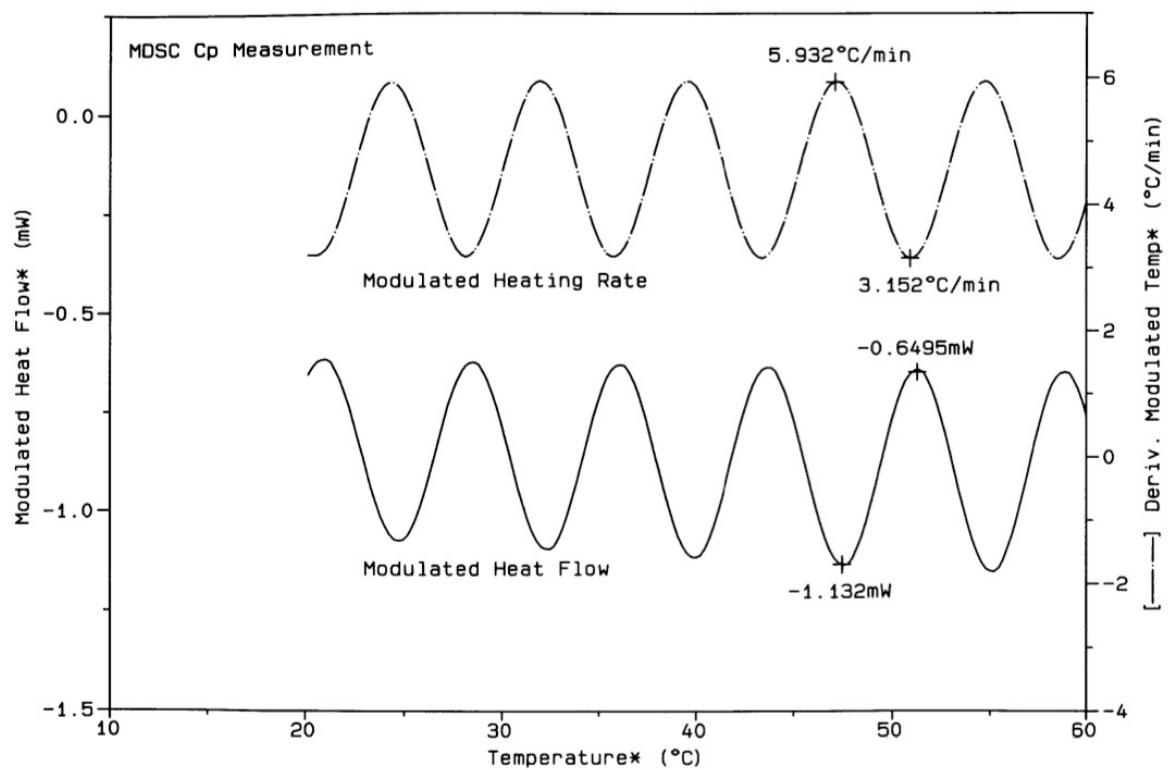


Figure 10: DSC & MDSC Cp MEASUREMENTS

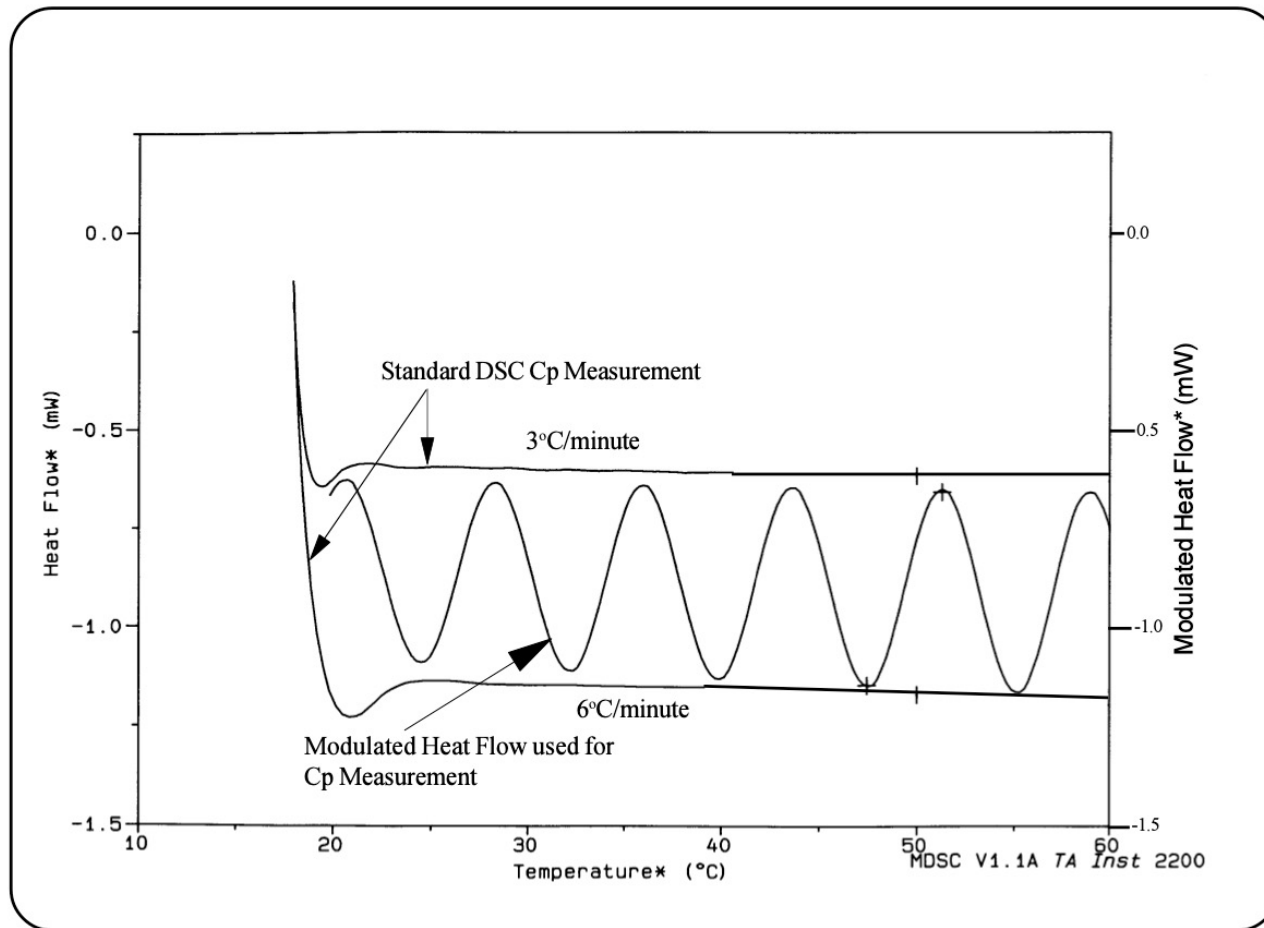


Figure 11: REVERSING HEAT FLOW FROM MDSC RAW SIGNALS

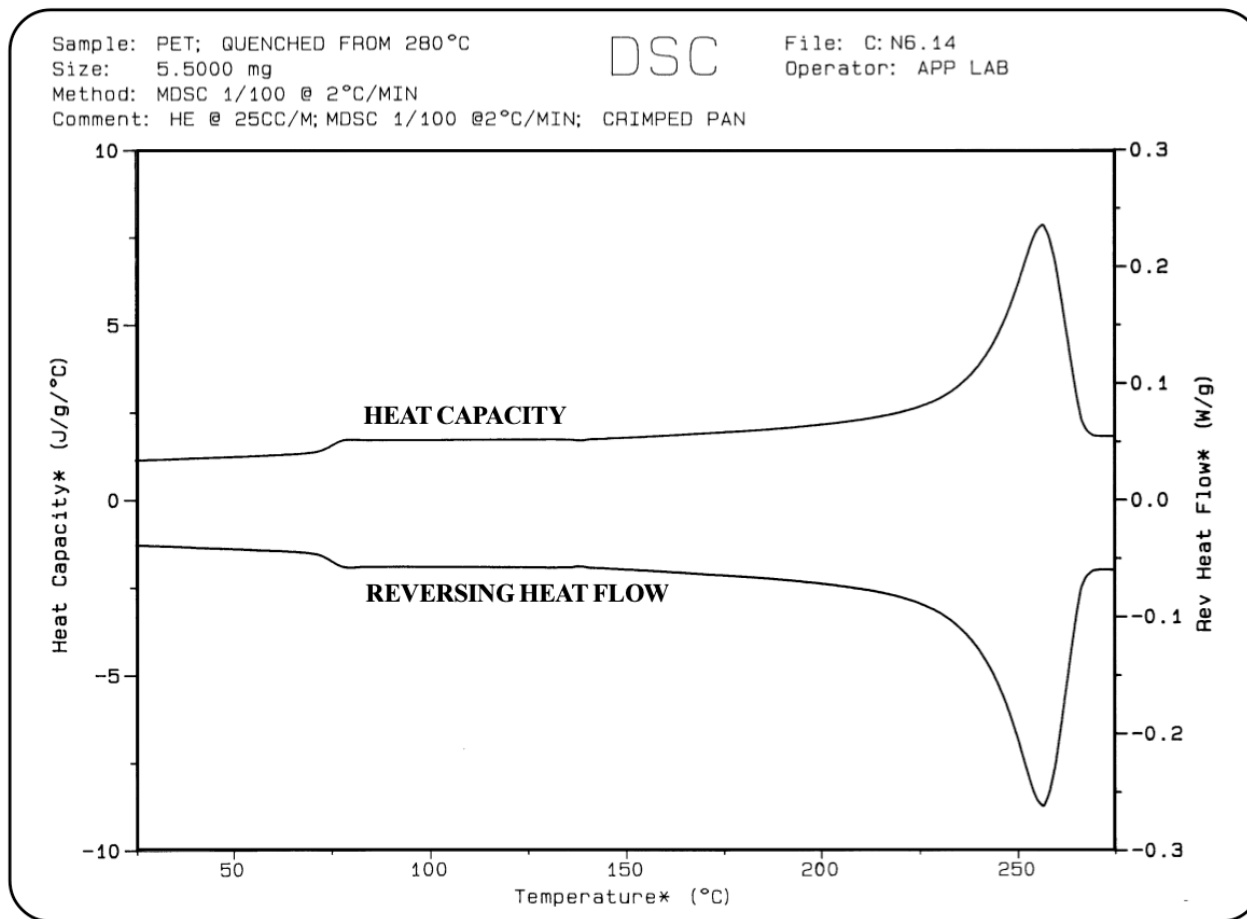


Figure 12: TOTAL HEAT FLOW FROM MDSC RAW SIGNALS

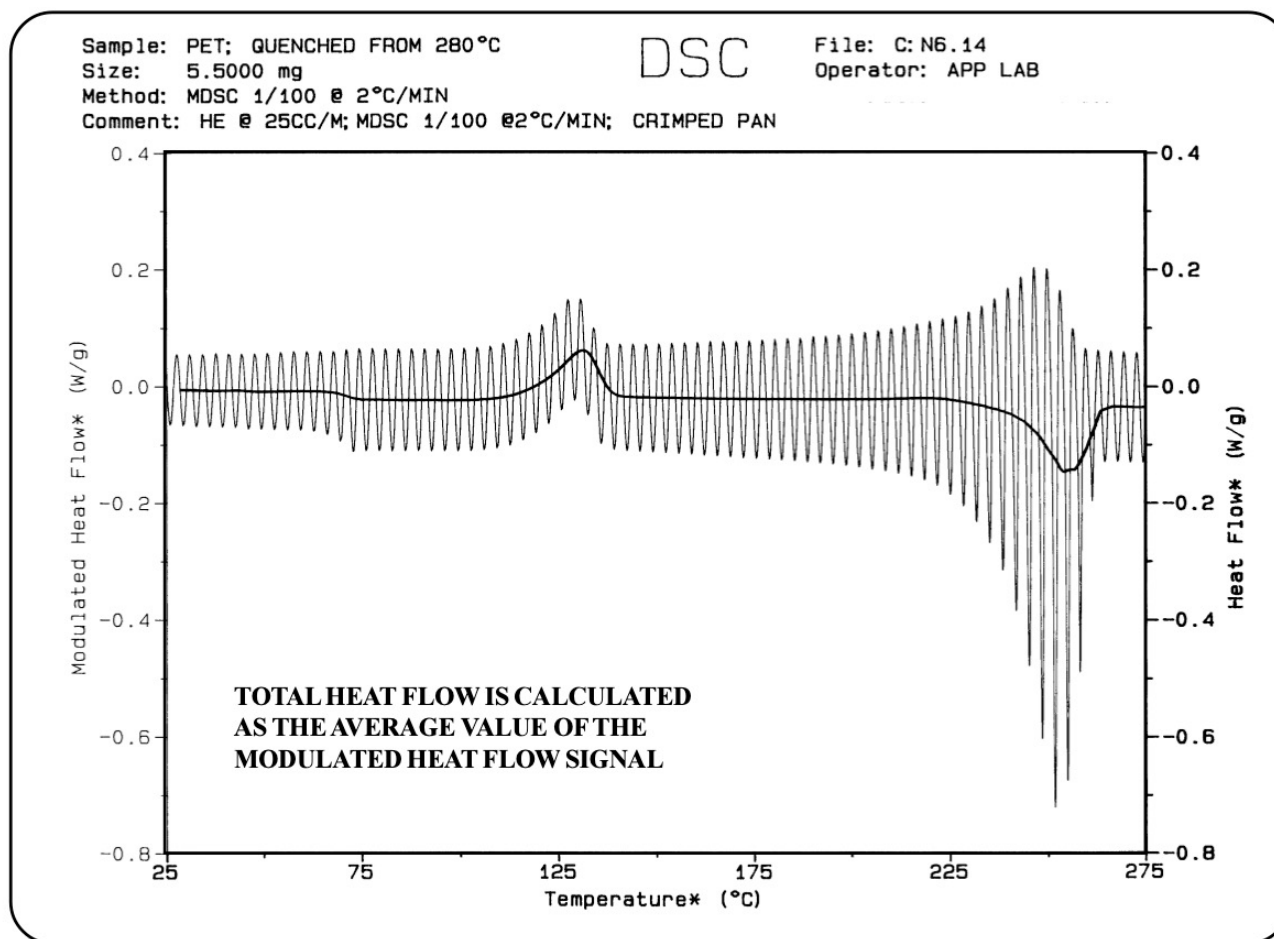
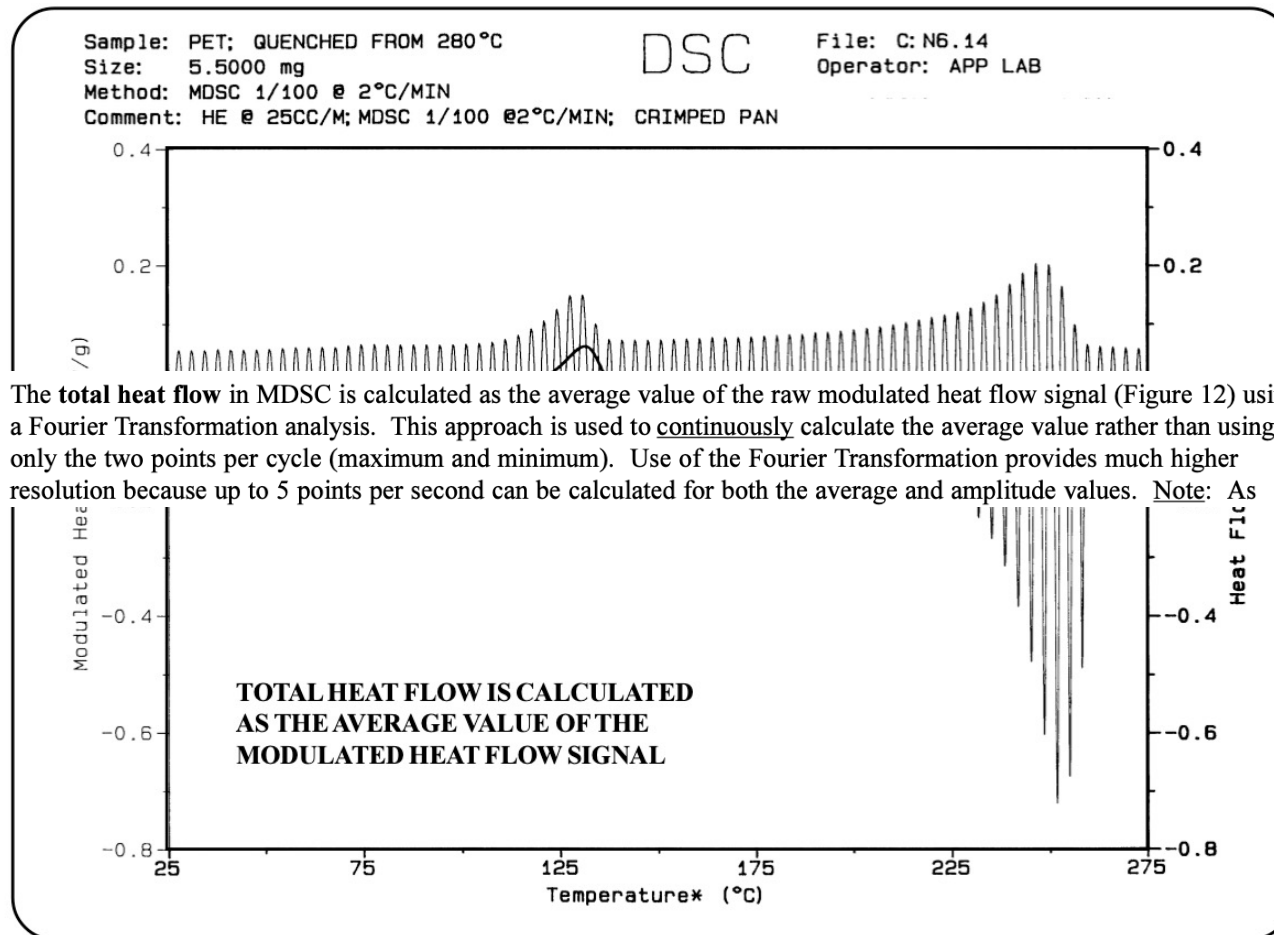


Figure 12: TOTAL HEAT FLOW FROM MDSC RAW SIGNALS



The **total heat flow** in MDSC is calculated as the average value of the raw modulated heat flow signal (Figure 12) using a Fourier Transformation analysis. This approach is used to continuously calculate the average value rather than using only the two points per cycle (maximum and minimum). Use of the Fourier Transformation provides much higher resolution because up to 5 points per second can be calculated for both the average and amplitude values. Note: As

Figure 13: QUENCH COOLED PET - MODULATED DSC

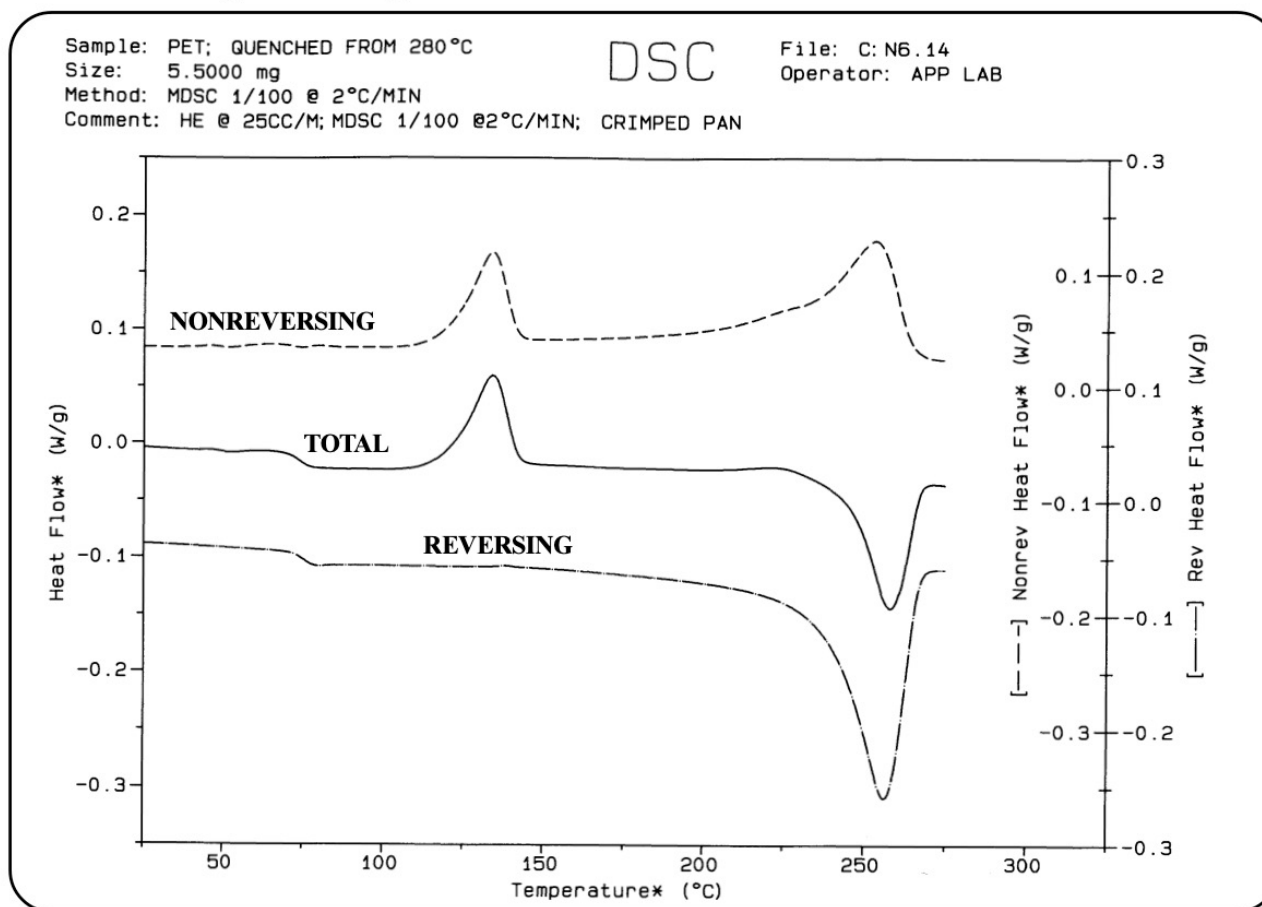


Figure 14: PHASE LAG

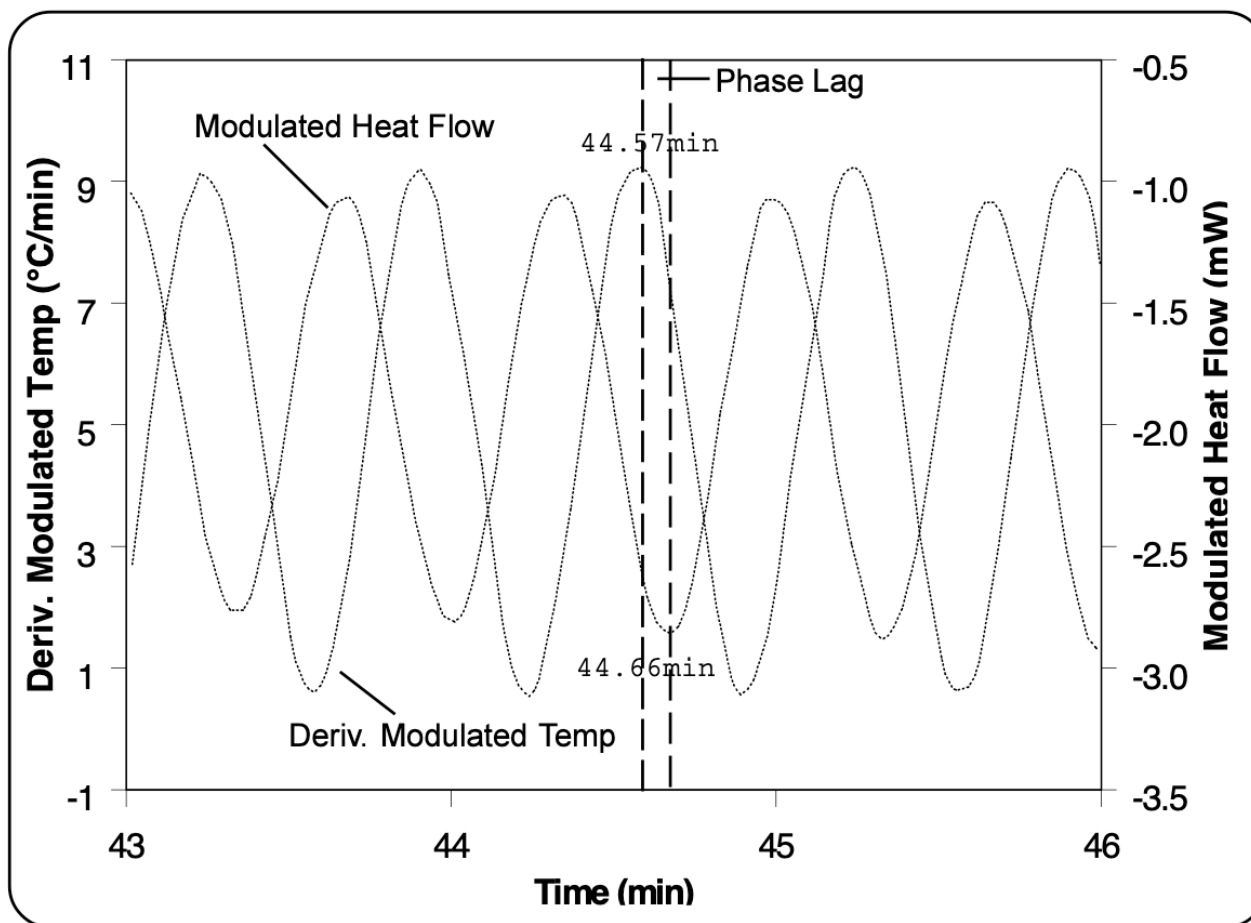
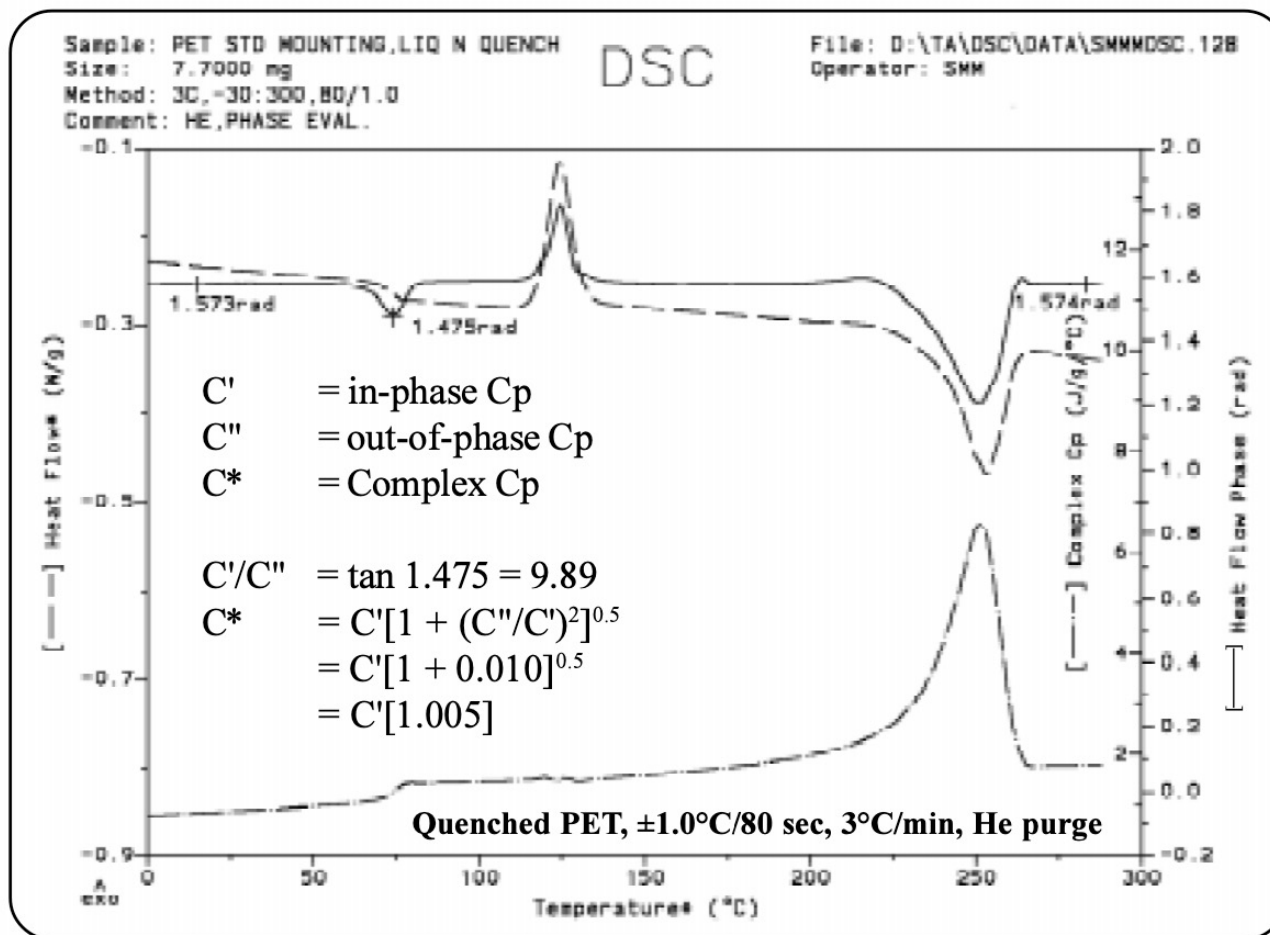
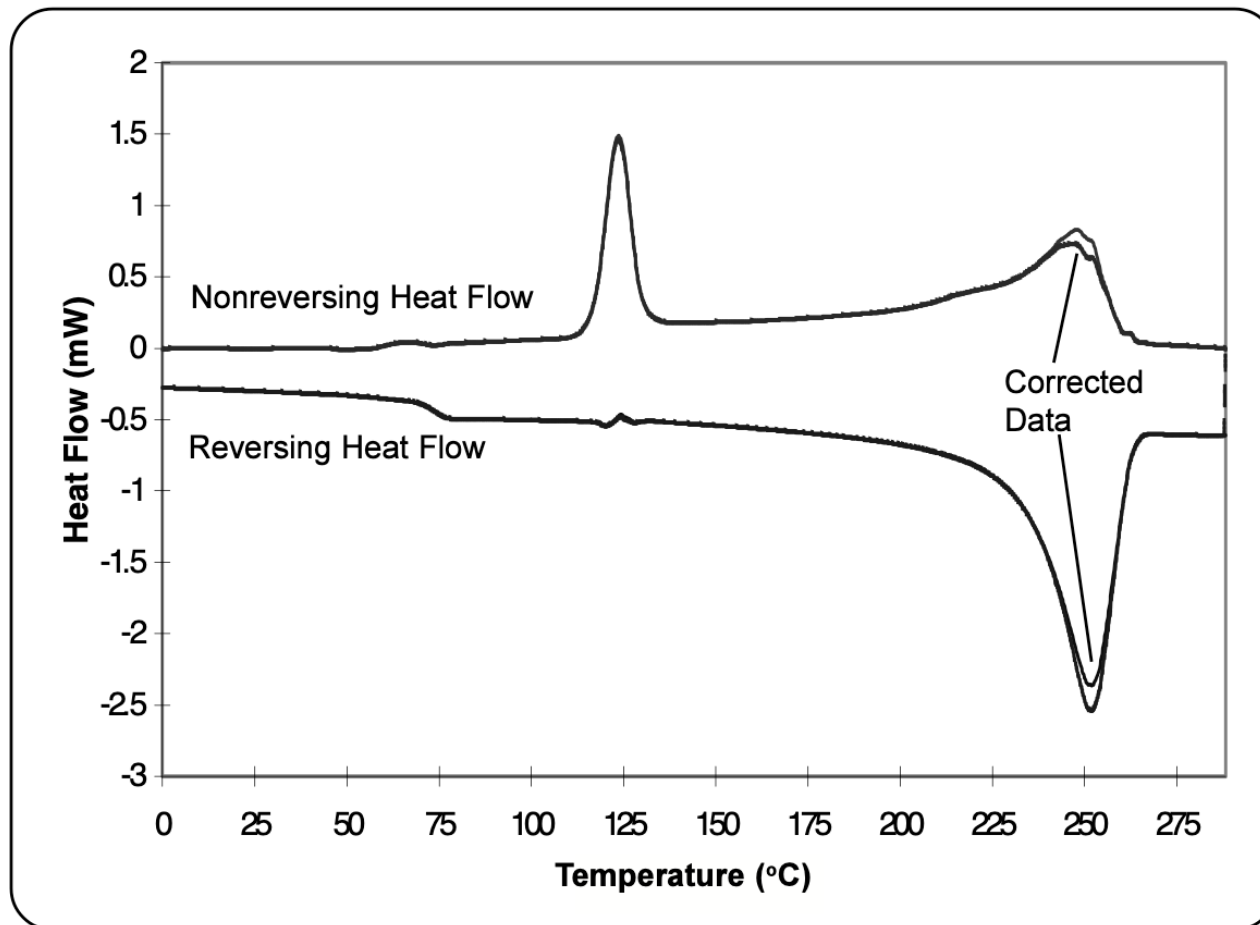


Figure 15: HEAT FLOW PHASE CONTRIBUTION



**Figure 16: PHASE-CORRECTED HEAT FLOW SIGNALS
QUENCHED PET**



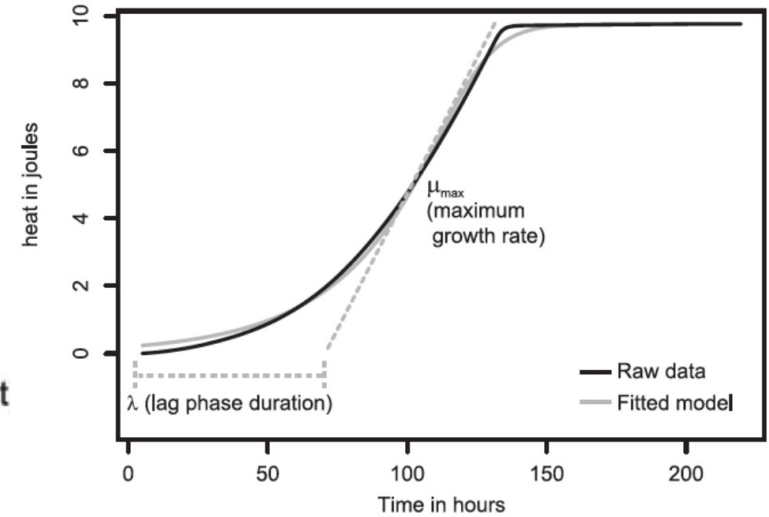
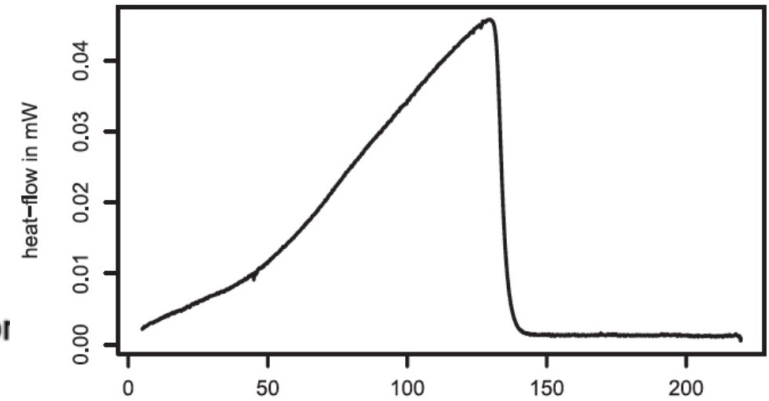
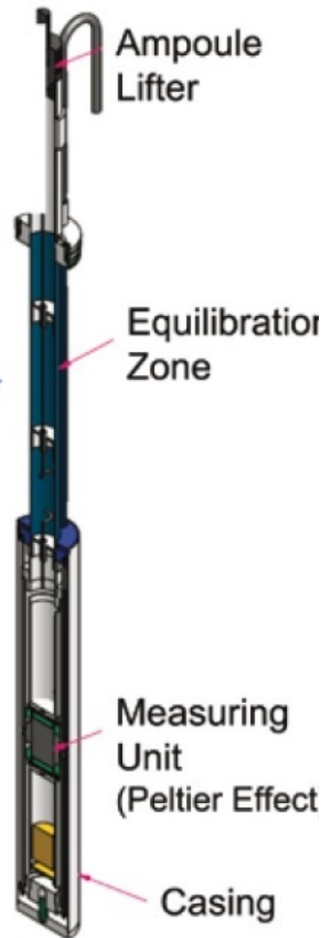
Micro Calorimetry (isothermal shown)

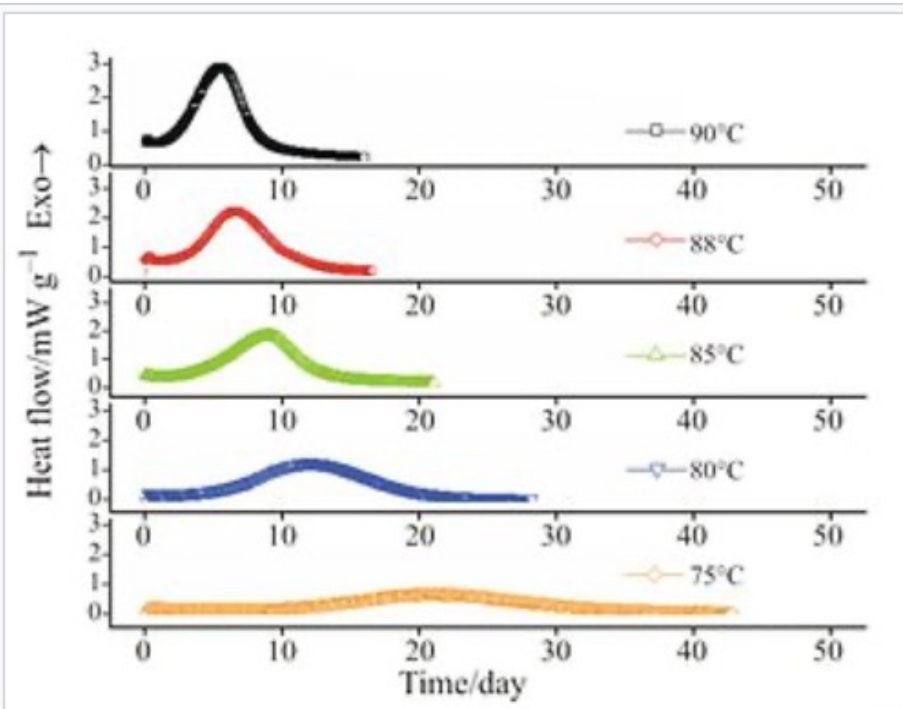
48 Channel Microcalorimeter



Specimen ampoule goes here: →

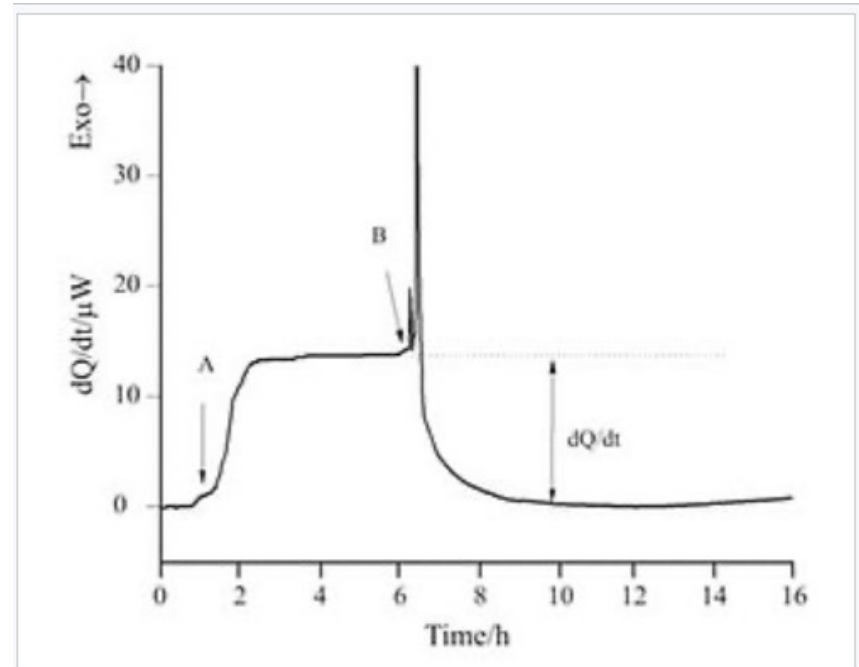
Heat flow measured relative to a reference: →



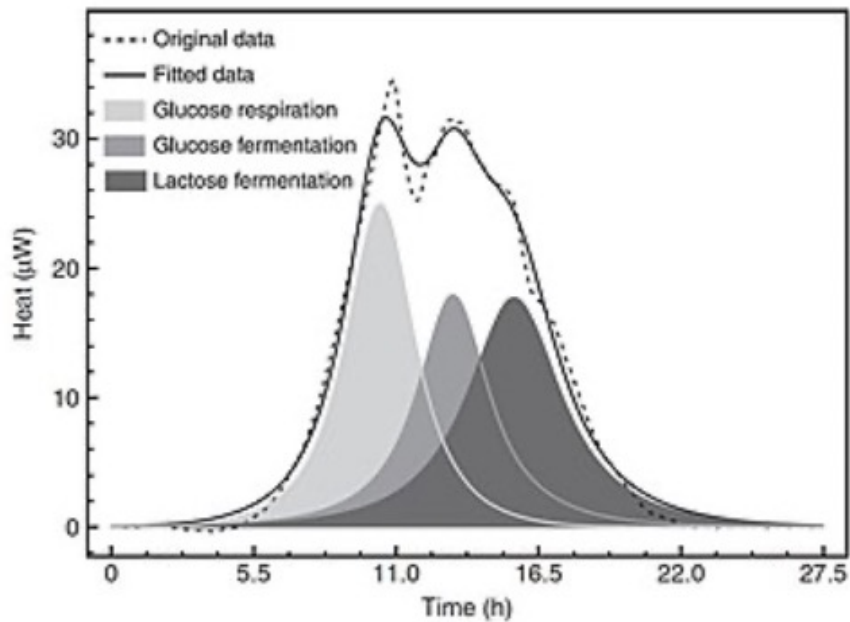


Heat flow vs. time for the thermal decomposition of 80 mass% CHP (cumene hydroperoxide) at a series of temperatures. CHP is an industrial chemical intermediate and polymerization initiator which is a documented fire and explosion hazard. According to the authors, neither differential scanning calorimetry or adiabatic calorimetry was sensitive enough to capture these data (from Chen et al. 2008 with publisher permission).

Fig. 4



Heat flow vs. time for the treatment of fibroblasts in culture in a stirred stainless steel ampoule. A = introduction of the ampoule into the measurement position, with metabolic heat flow then reaching an equilibrium level. B = injection of sodium dodecyl sulfate (SDS) which produced sharp heat flow peaks related to exothermic dilution of the SDS and lysis of the fibroblasts. After lysis, the heat flow rate returned near zero since fibroblast metabolism had ceased. dQ/dt = the metabolic heat flow of the fibroblasts in culture (from Liu, et al. 2007 with publisher permission). Fig. 5



Example of how growth-related heat flow vs. time data from bacteria in culture in a given medium in a sealed ampoule reflect the sequence of metabolic activities taking place. The bacteria move on to consuming less efficient carbon sources as more efficient sources are depleted. Deconvolution of the data yielded the peaks shown which can be assigned to the metabolic modes shown. This sequence for the *E. coli* bacteria employed is well known in the field of microbiology (from Braissant et al. 2010 with publisher permission). Fig.6

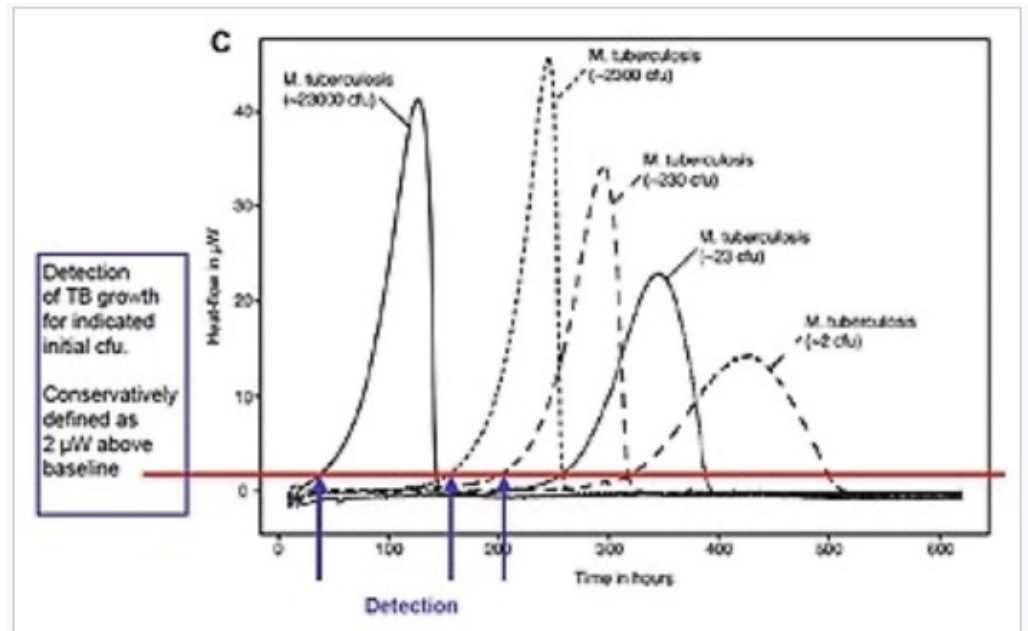


Illustration of how IMC time of detection of the presence of bacteria depends on the initial number of bacteria present (CFU), the sensitivity of the instrument and the level of heat flow above baseline that is selected as indicating bacterial growth. CFU = colony forming unit. (adapted from Braissant et al. 2010 with publisher permission). Fig.7

Thermogravimetric Analysis (TGA)



Thermogravimetric Analysis (TGA)

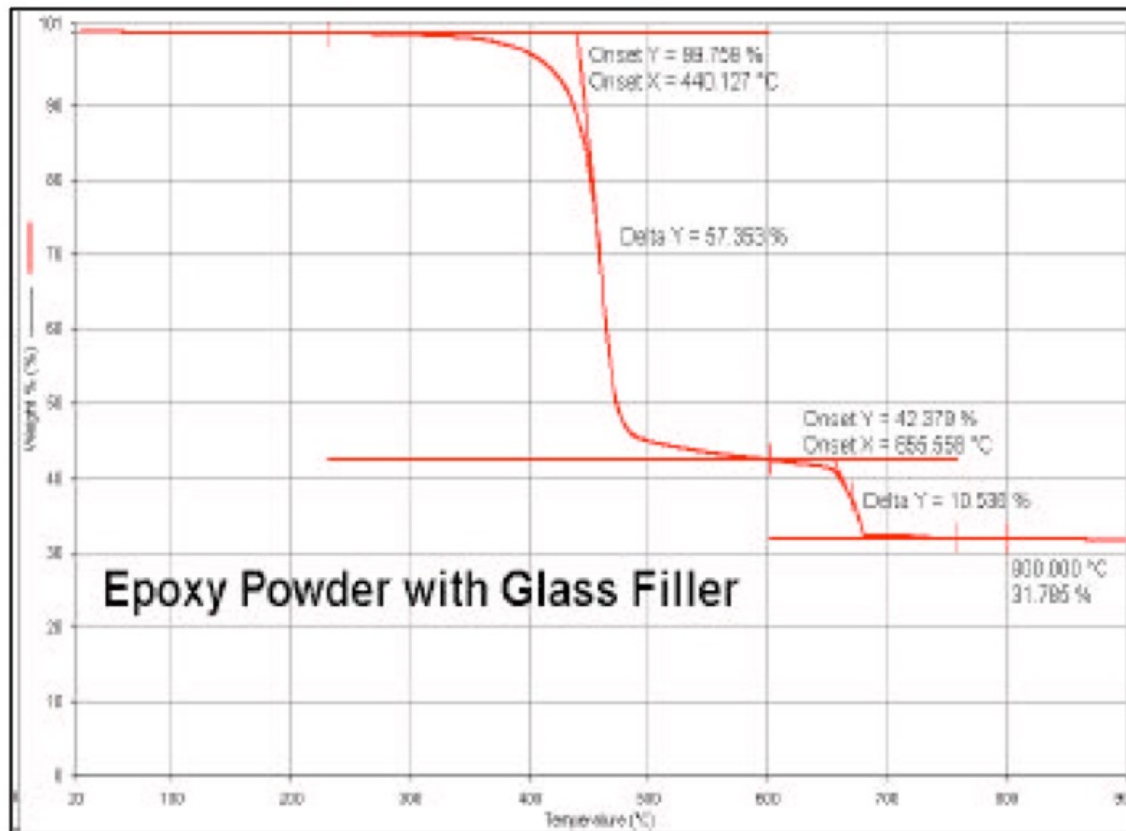


Figure 3. TGA results for epoxy-glass powder

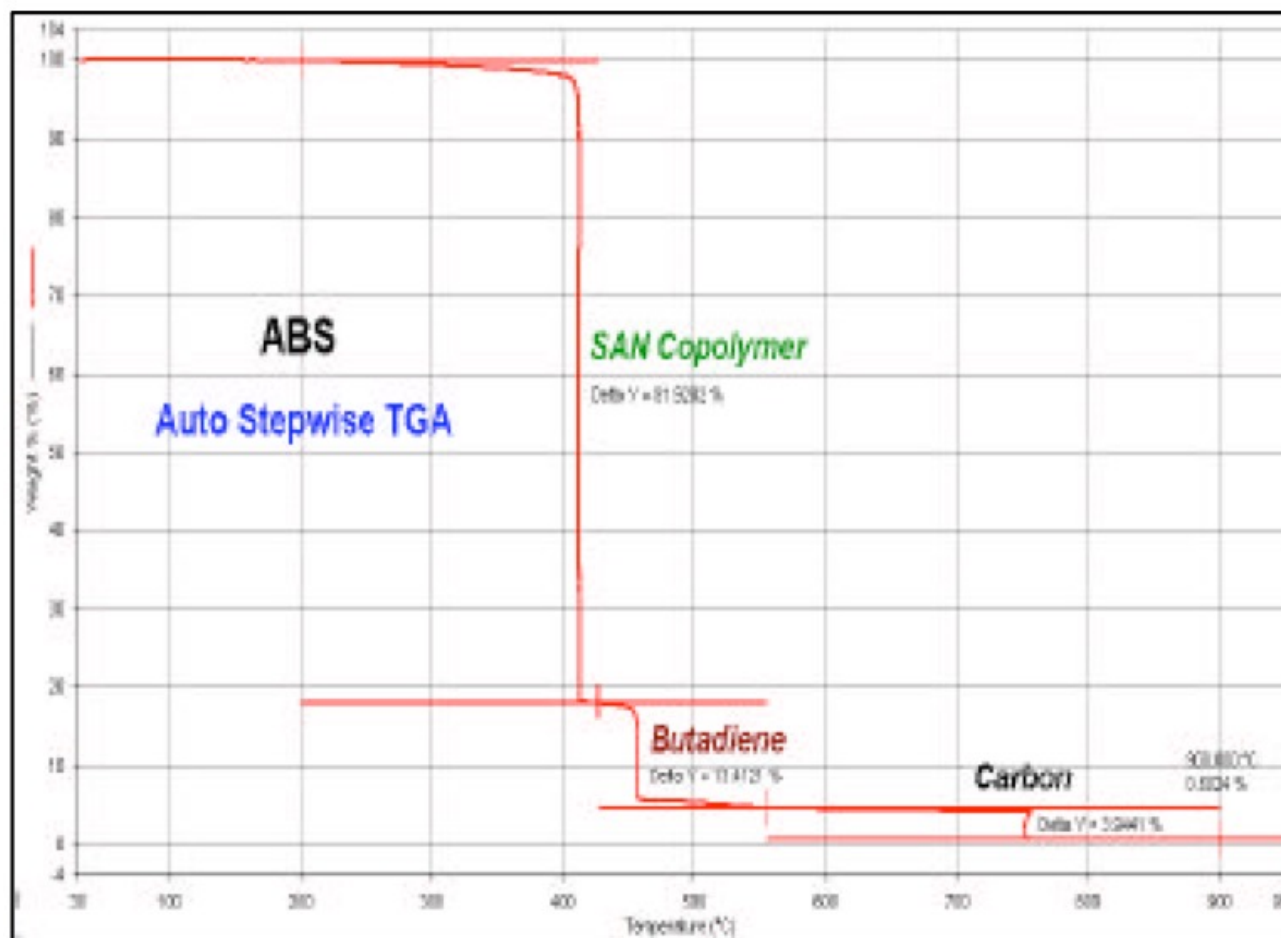


Figure 5. Auto Stepwise TGA results for ABS showing separation of SAN and butadiene components

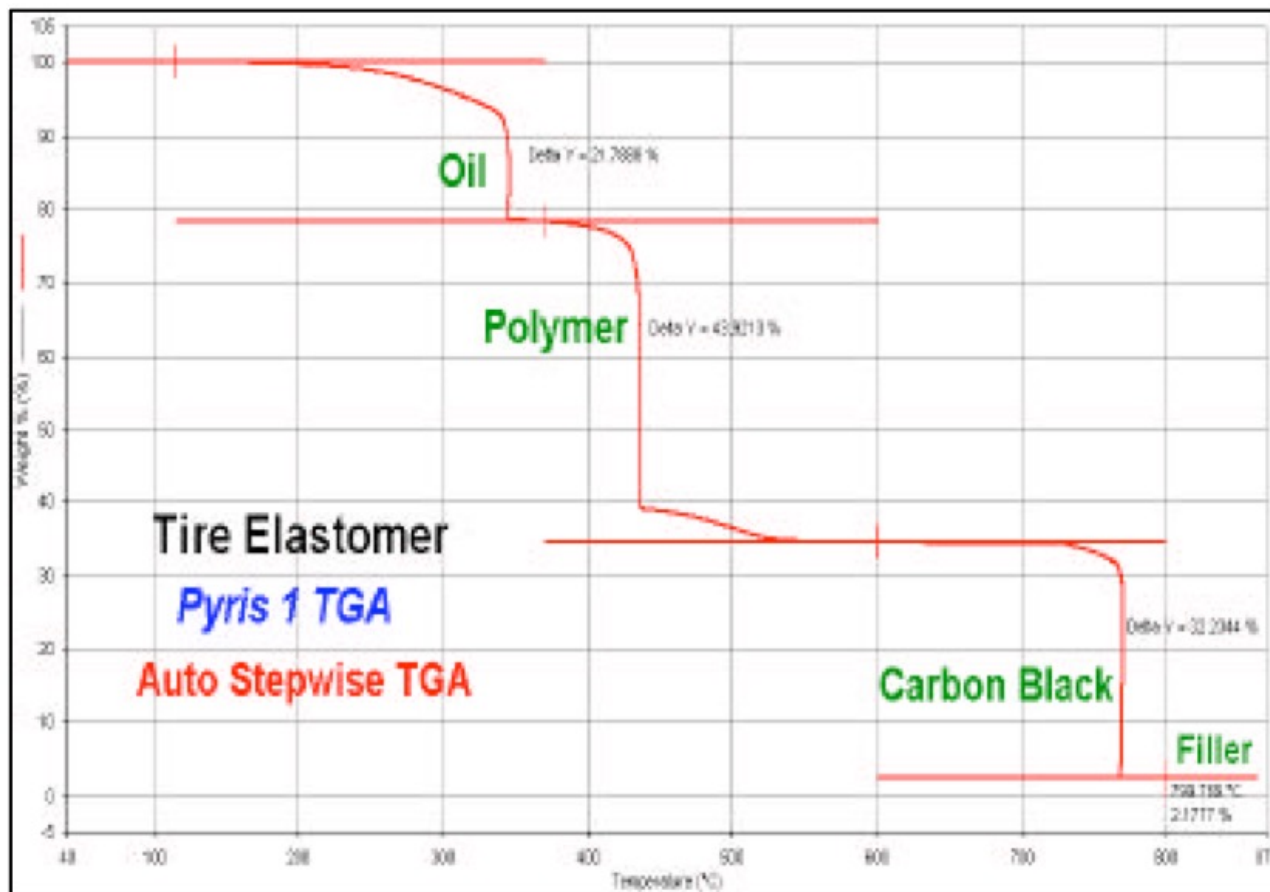


Figure 6. Auto Stepwise TGA compositional results for tire elastomer showing separation of oil, polymer, carbon black and filler

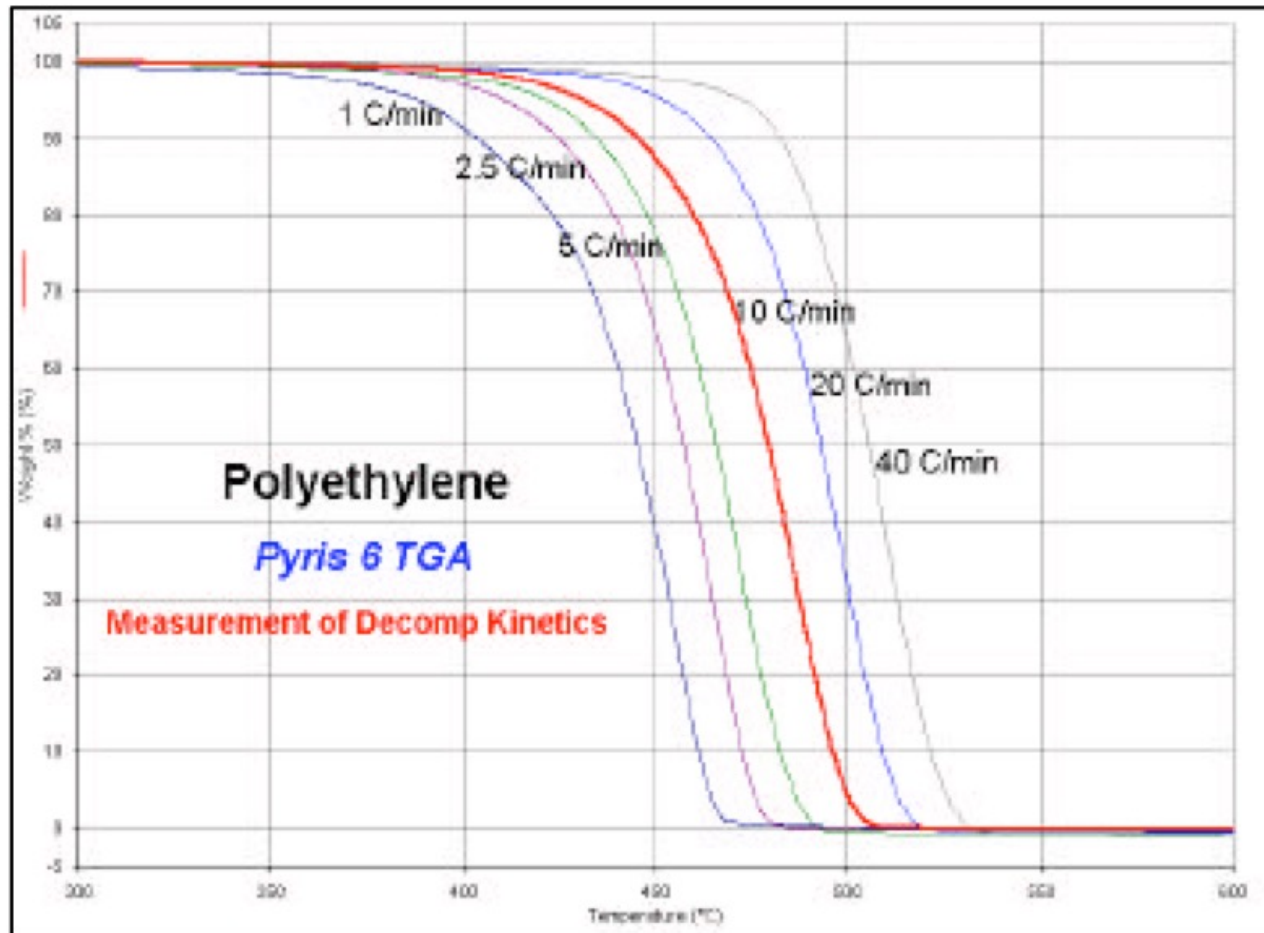
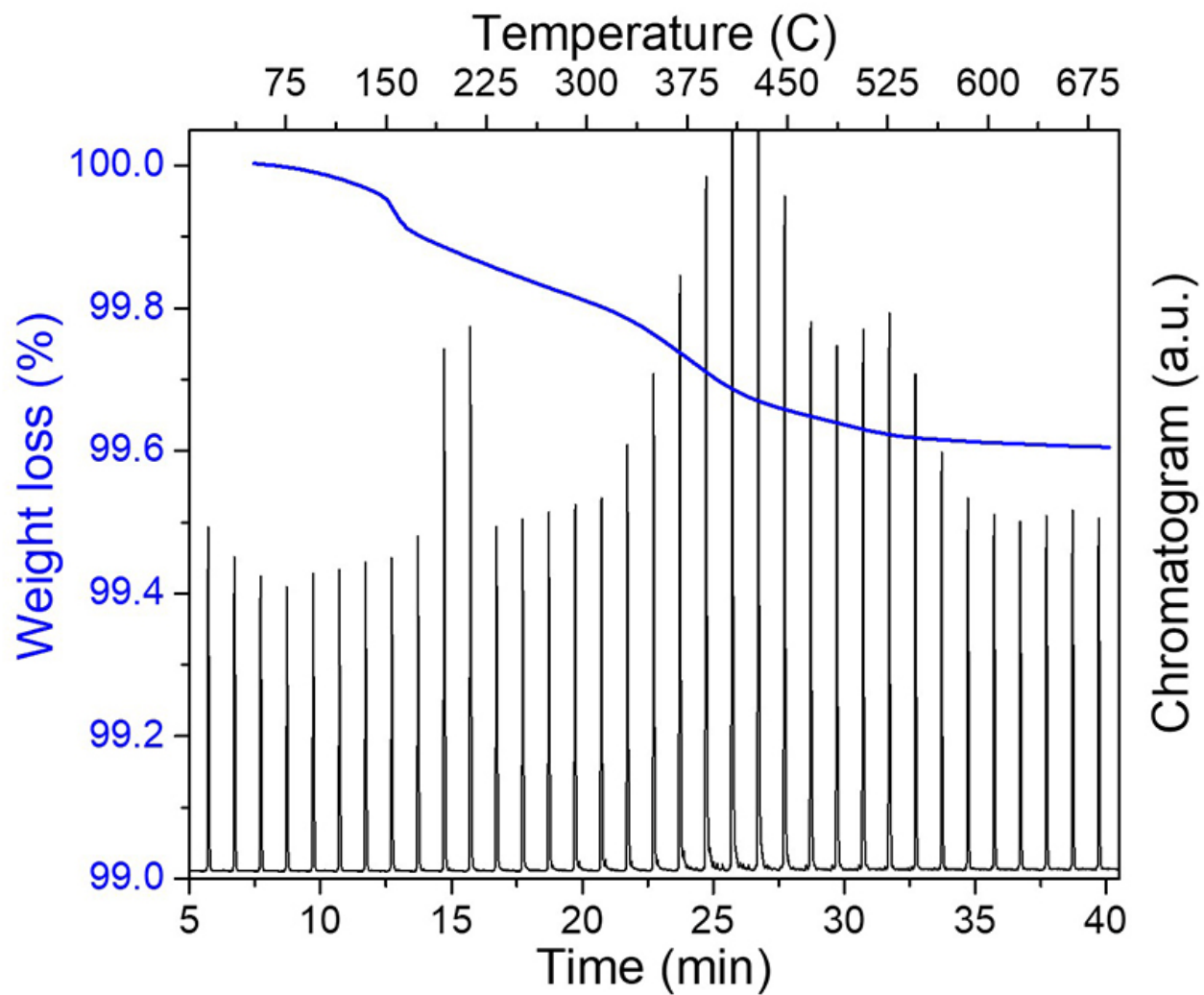


Figure 8. Effect of heating heat on thermal decomposition of polyethylene



TGA/MS
GC
IR
Raman
Etc.

Example of TGA coupled with GC-MS showing the identification of different ions released by the material as a function of temperature

Membrane Osmometry

In an ideally dilute solution, **van 't Hoff's law of osmotic pressure** can be used to calculate M_n from osmotic pressure.^[1]

$$\lim_{c \rightarrow 0} \left(\frac{\Pi}{c} \right) = \frac{RT}{M_n}$$

M_n , number average molecular weight, mass/mole

R , **gas constant**

T , **absolute temperature**, typically Kelvin

c , concentration of polymer, mass/volume

Π , osmotic pressure

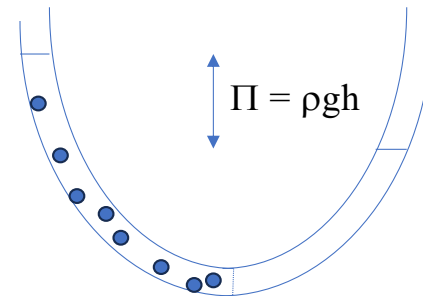
$$\frac{\pi}{c} = RT \left(\frac{1}{M_n} + A_2 c + \dots \right)$$

$$A_2 = \frac{1}{M^2} \left(b - \frac{a}{RT} \right)$$

Van der Waals

b = Excluded volume

a = attractive potential



Van der Waals Equation $P = \Pi$

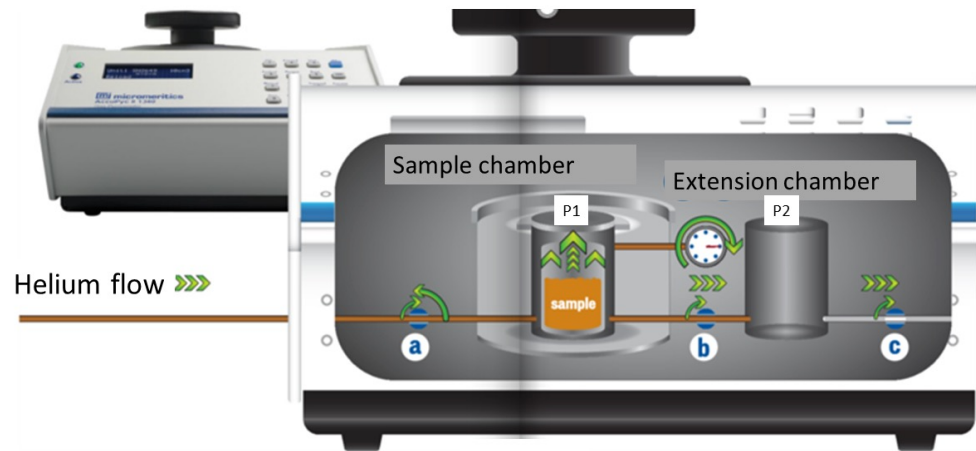
$$P = \frac{RT}{V - b} - \frac{a}{V^2}$$

Archimedes Method for Density

$$\frac{\text{density of object}}{\text{density of fluid}} = \frac{\text{weight}}{\text{weight of displaced fluid}}$$

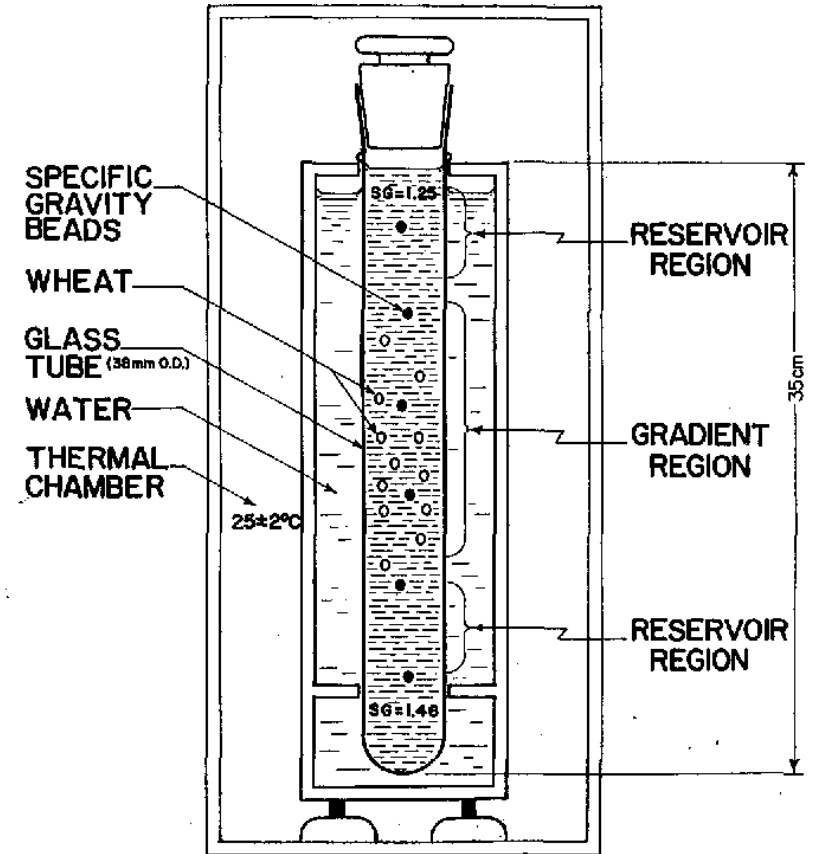
Helium Pycnometry

- Helium density
- Boyle's Law ($P_1V_1 = P_2V_2$)
- Measure pressure change to get volume
- Weigh sample
- “Open pore” density



$$V_{\text{sample}} = V_{\text{sample chamber}} - \frac{V_{\text{expansion chamber}}}{\frac{P_1}{P_2} - 1} \quad D_{\text{sample}} = \frac{M_{\text{sample}}}{V_{\text{sample}}}$$

Density Gradient Column



Mercury Dilatometry for Thermal Expansion Coefficient, α

$$\alpha = \frac{1}{V} \left(\frac{\partial V}{\partial T} \right)_{p,N}$$



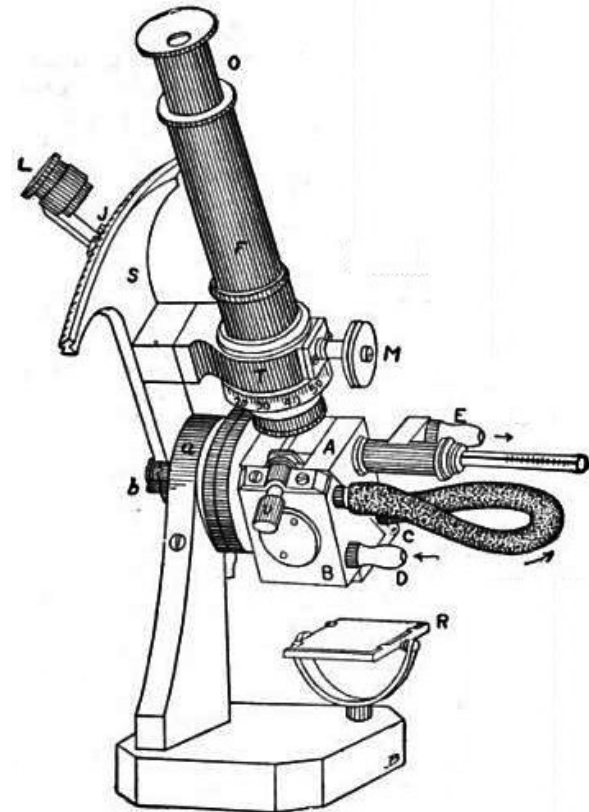
Abbe Refractometer

$$n = \frac{C}{v}$$

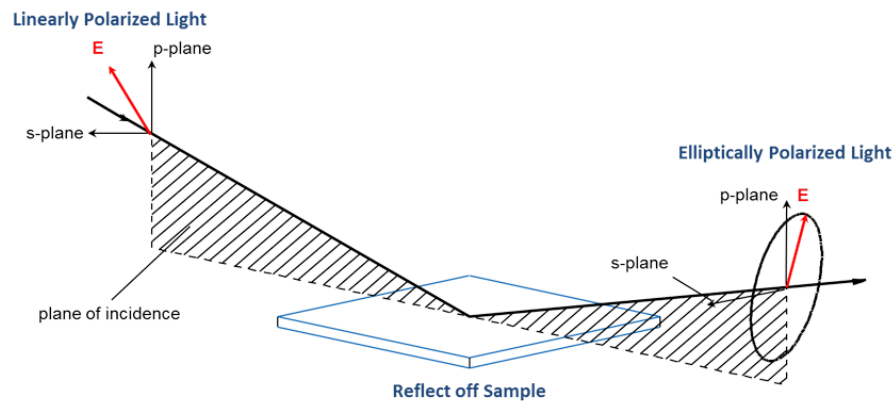
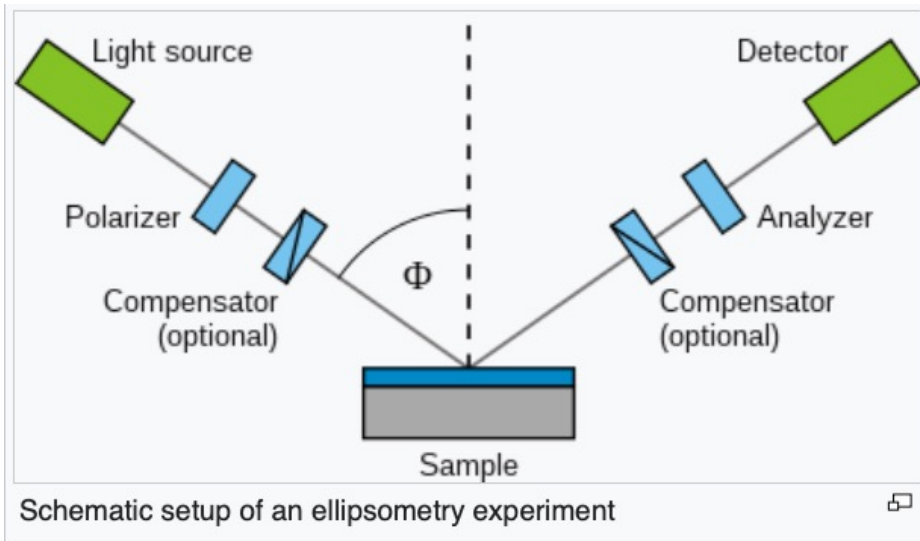
sion of free volume above T_g . Under the assumption of a spherical molecule, the density ρ can be related to the index of refraction n by using the Lorentz-Lorenz equation,

$$\frac{(n^2 - 1)}{(n^2 + 2)} = \rho C \quad (2)$$

where C is the specific refraction, which depends on the polarizability of the molecules (temperature independent).¹⁹ Equation (2) results in a monotonically decreasing index of refraction with decreasing density.



Index (and thickness) of thin films Ellipsometer



The illustration to the right represents a generic volumetric physical adsorption analyzer in its most elementary form. The critical components are:

- 1) Analysis manifold of accurately known volume and temperature
- 2) Vacuum system with valve to manifold
- 3) Source of adsorptive gas (typically, N_2) with valve to manifold
- 4) Pressure transducer and temperature sensor
- 5) Means for recording the signal from the transducer and temperature sensor
- 6) A sample tube of precisely known free or void-space
- 7) Sample tube connected to analysis manifold
- 8) Means to reduce the temperature of the sample when required, (typically to liquid nitrogen (LN_2) temperature).

Preparation

The adsorptive gas supply valve (3) is closed and the vacuum (2) and sample (7) valves are open allowing the manifold and sample tube to be evacuated. The sample tube is not in the cold bath, so the sample is at ambient temperature.

When the necessary vacuum is achieved, valves 2 and 7 close and the cold bath is raised, cooling the sample to the analysis temperature.

Charging the Manifold

Valve 3 is opened momentarily to charge the manifold to a pressure (P_m) slightly above vacuum, preparing the instrument to dispense a dose of adsorptive onto the sample. The quantity of gas (n_m) in the manifold can be determined from the universal gas law

$$n_m = \frac{P_m V_m}{RT}$$

Surfaces: Gas Adsorption

Dosing

Valve 7 is opened allowing some of the gas to enter the sample tube.

Equilibration

Some quantity of gas (n_{ads}) will be adsorbed by the sample and removed from the gas phase. Pressure is monitored until it stabilizes, indicating adsorption has equilibrated. The equilibration pressure (P_e) is recorded.

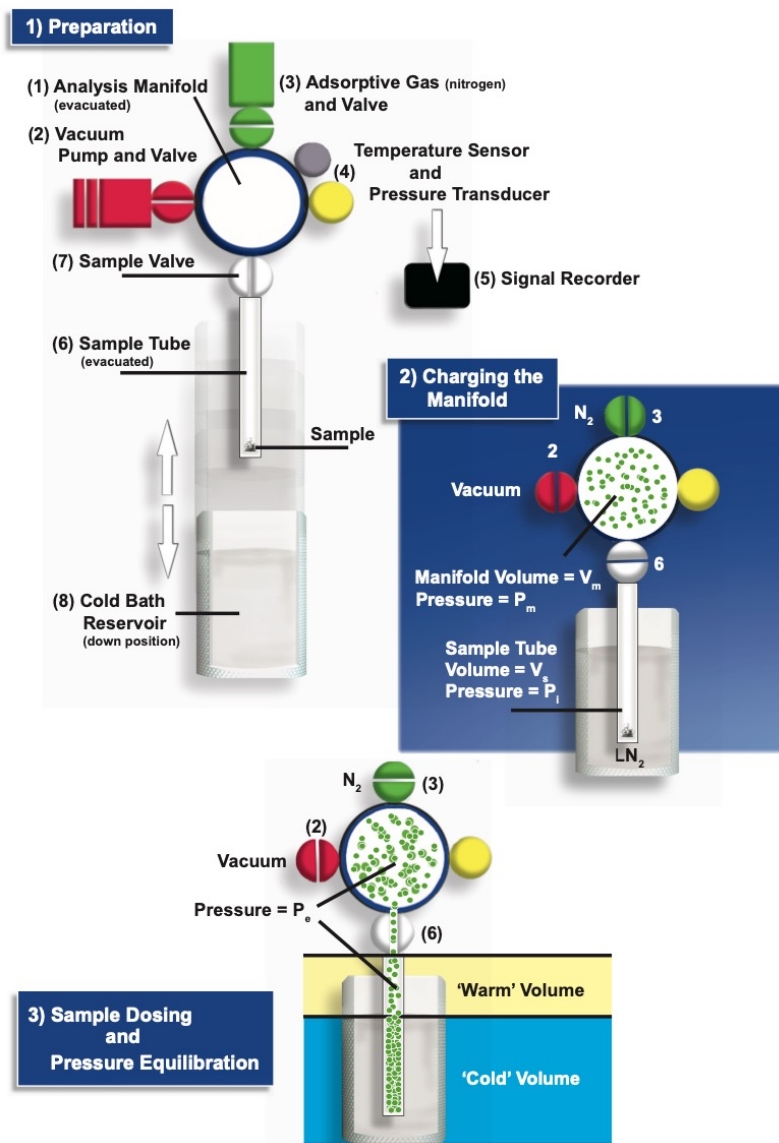
Quantity Adsorbed

The quantity of gas (n_e) remaining in the combined manifold and sample tube volume ($V_m + V_s$) can be calculated from the universal gas law. This is complicated by the vertical temperature profile in the sample tube, one portion essentially being at ambient temperature and another portion being at the temperature of the cold bath typically LN_2 .

The calculation of n_e is made traceable by a free-space measurement typically performed prior to the analysis and which characterizes the sample tube volume in regard to 'warm' and 'cold' volumes. Once n_e is determined, the quantity of gas adsorbed by the sample at P_e is

$$n_{ads} = n_m - n_e$$

This establishes the point on the isotherm (P_e, n_{ads}). Valve 7 closes and valve 3 opens, and the manifold is charged to a pressure slightly higher than P_e after which the dosing and equilibration processes are repeated.



Quantity Adsorbed

The quantity of gas (n_g) remaining in the combined manifold and sample tube volume ($V_m + V_s$) can be calculated from the universal gas law. This is complicated by the vertical temperature profile in the sample tube, one portion essentially being at ambient temperature and another portion being at the temperature of the cold bath typically LN_2 .

The calculation of n_g is made traceable by a free-space measurement typically performed prior to the analysis and which characterizes the sample tube volume in regard to 'warm' and 'cold' volumes. Once n_g is determined, the quantity of gas adsorbed by the sample at P_c is

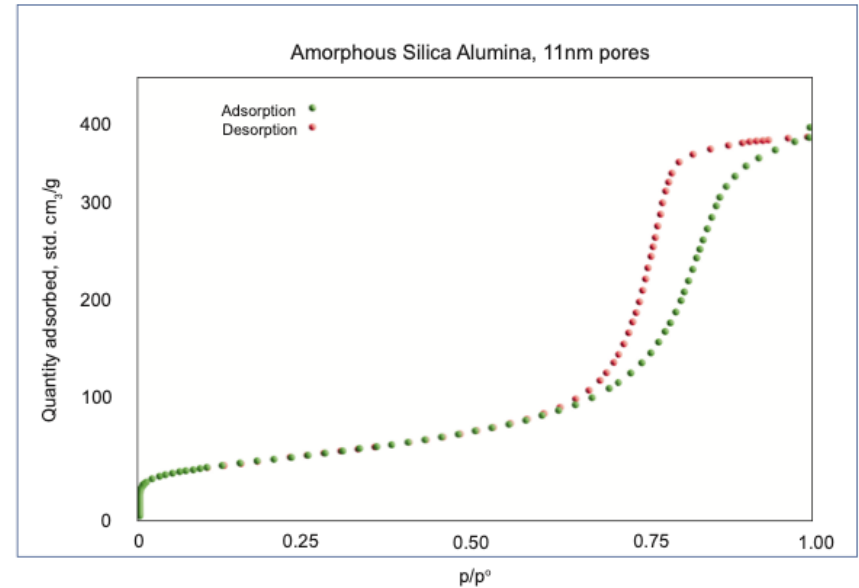
$$n_{\text{ads}} = n_m - n_c$$

This establishes the point on the isotherm (P_c, n_{ads}). Valve 7 closes and valve 3 opens, and the manifold is charged to a pressure slightly higher than P_c after which the dosing and equilibration processes are repeated.

This cycle continues until the analysis pressure is near saturation pressure at which time the complete adsorption isotherm has been developed. The desorption isotherm is measured by a step-wise reduction in pressure until a low pressure over the sample is achieved. At that point, most of the physically adsorbed molecules will have been desorbed from the surface.

Type IV isotherm:

Nitrogen adsorption and desorption on amorphous silica alumina.



X-ray and Neutron Reflectivity

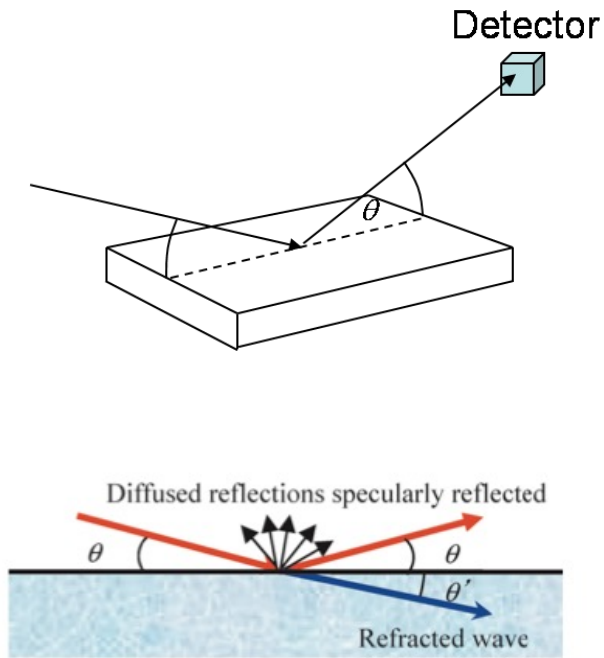
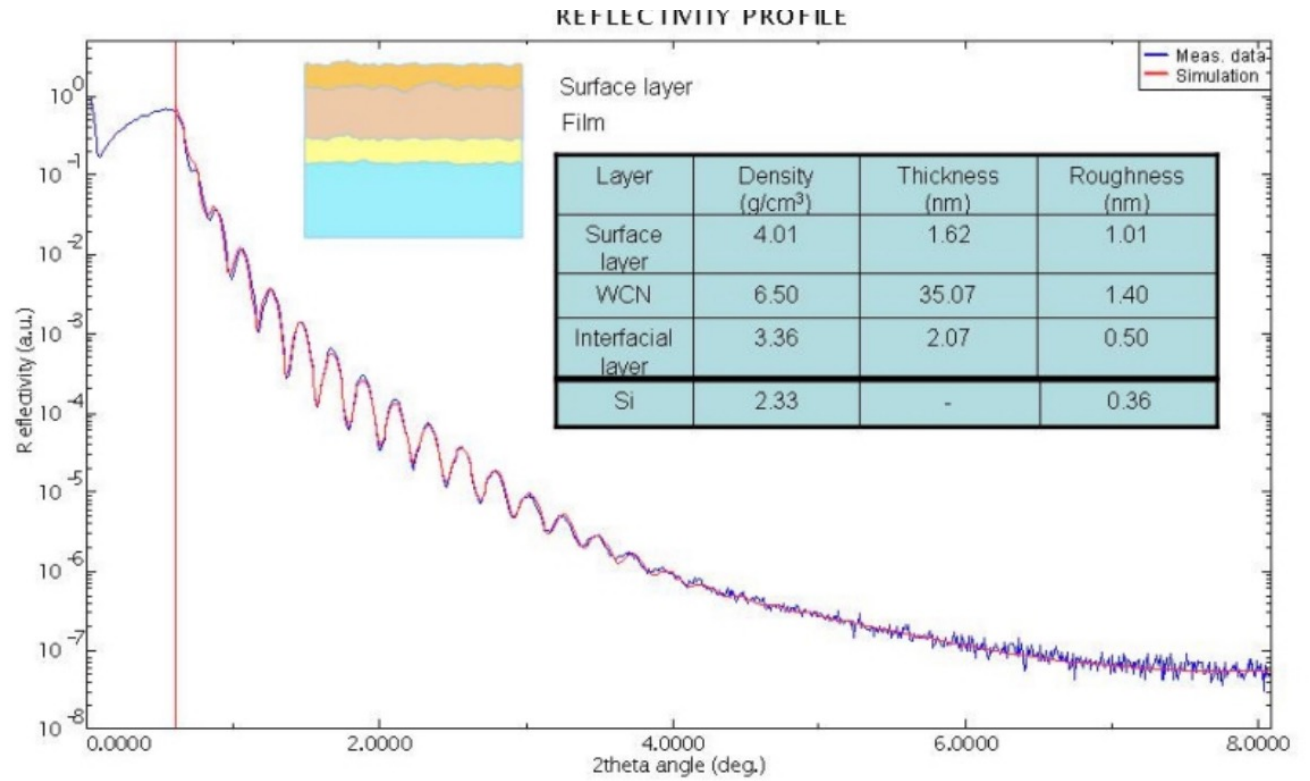


Fig. 1. Reflection and refraction of X-rays on material surface.



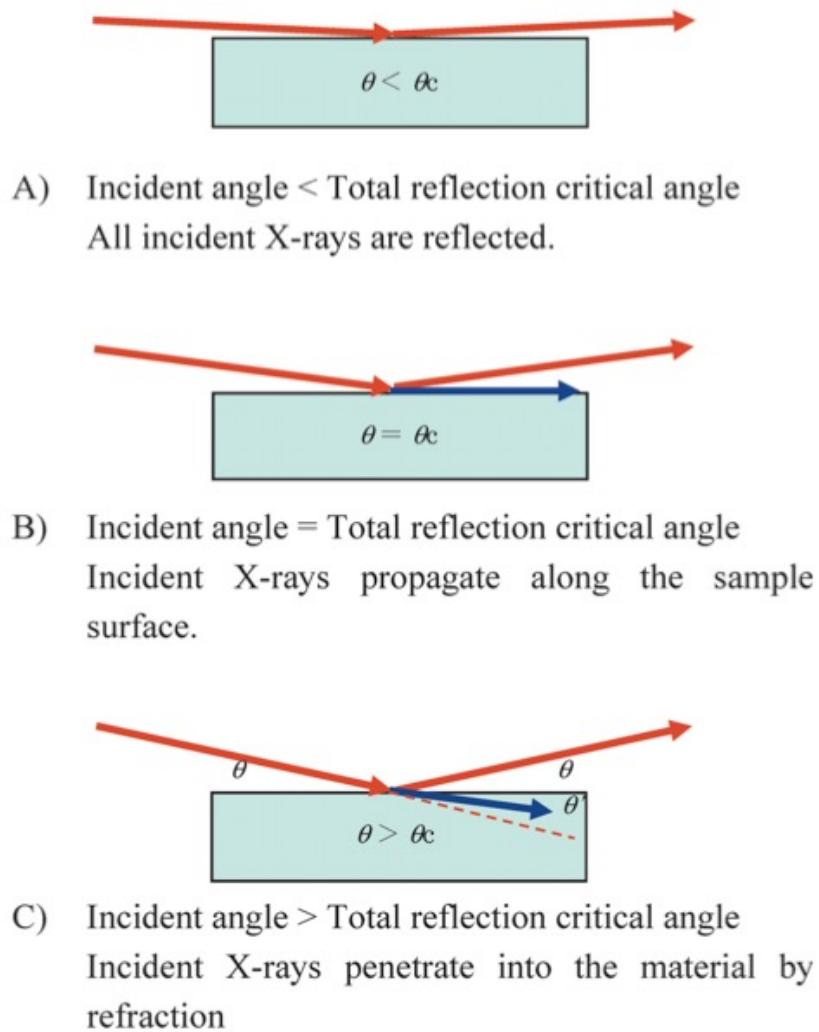


Fig. 3. Reflection and refraction of X-rays at material surface with the changes in the grazing angle.

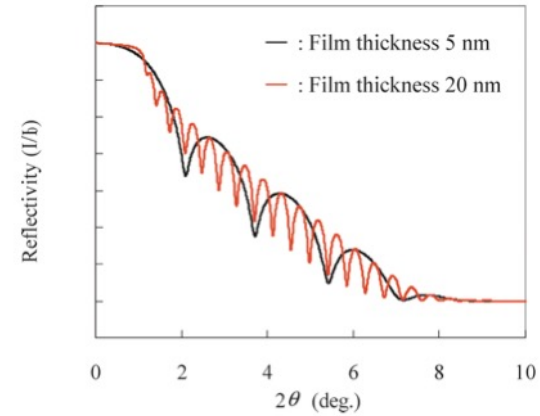


Fig. 4. Reflectivity of Au film on Si substrate.

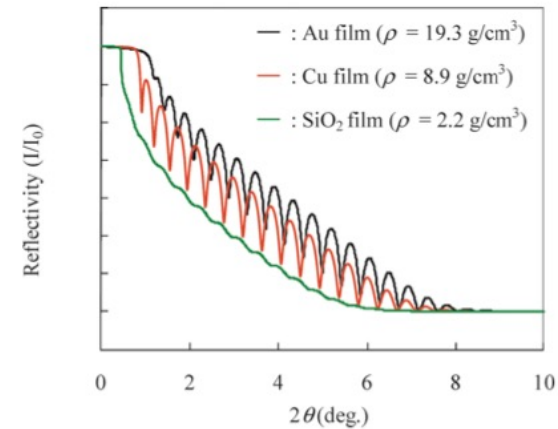


Fig. 5. X-ray reflectivity curves of Au, Cu and SiO₂ film on Si substrates (film thickness is 20 nm).

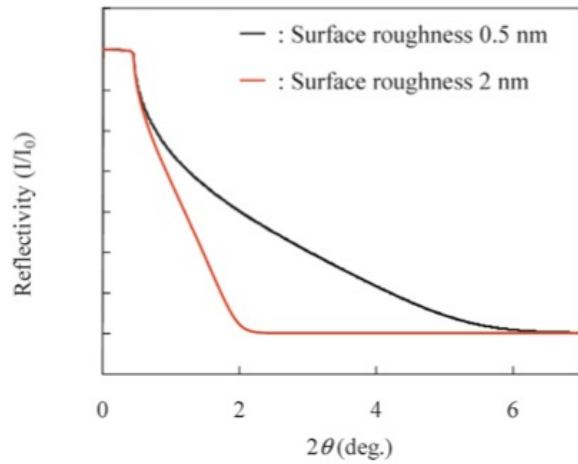


Fig. 6. X-ray reflectivity curves of Si substrates with two different values of surface roughness.

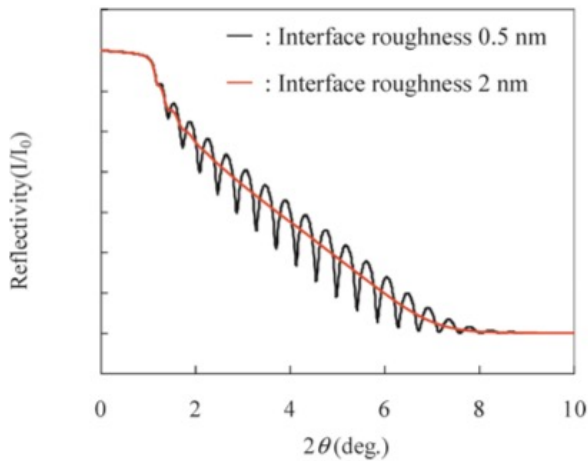


Fig. 7. X-ray reflectivity of Si substrate differences with interface roughness (Film thickness is 20 nm).

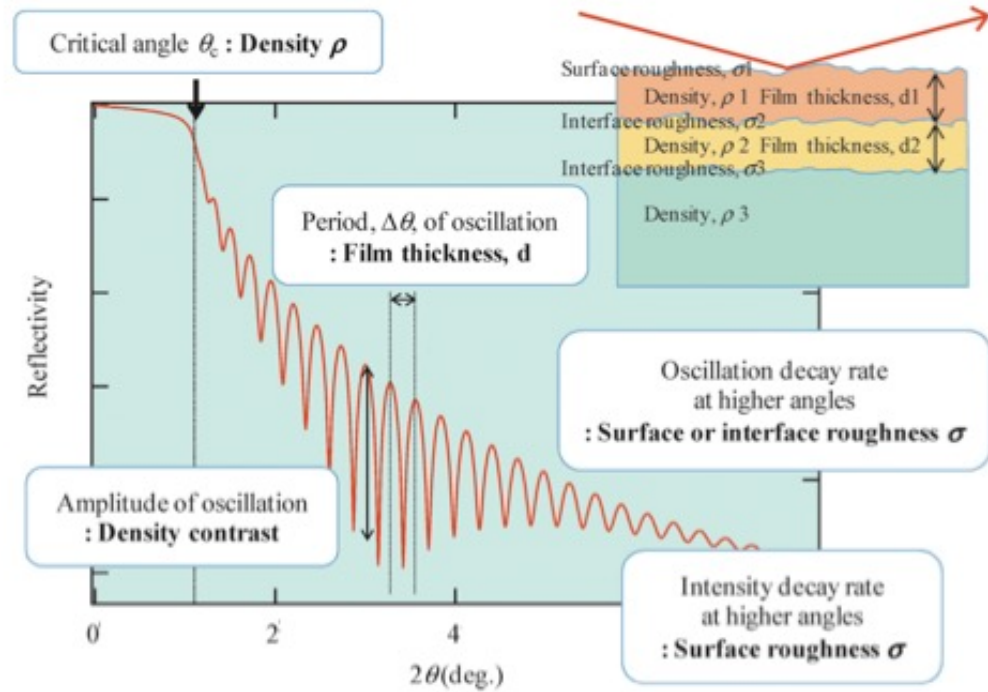
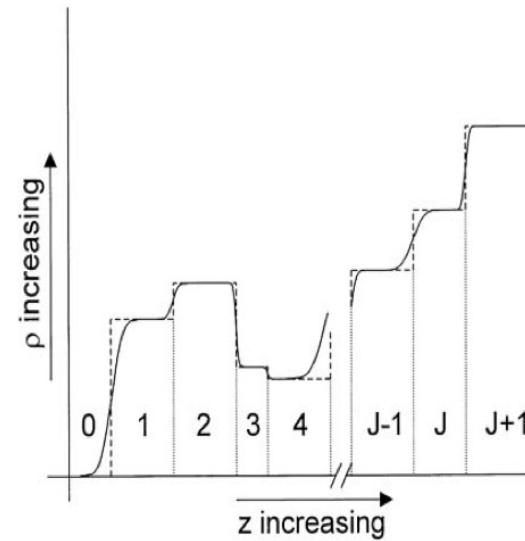
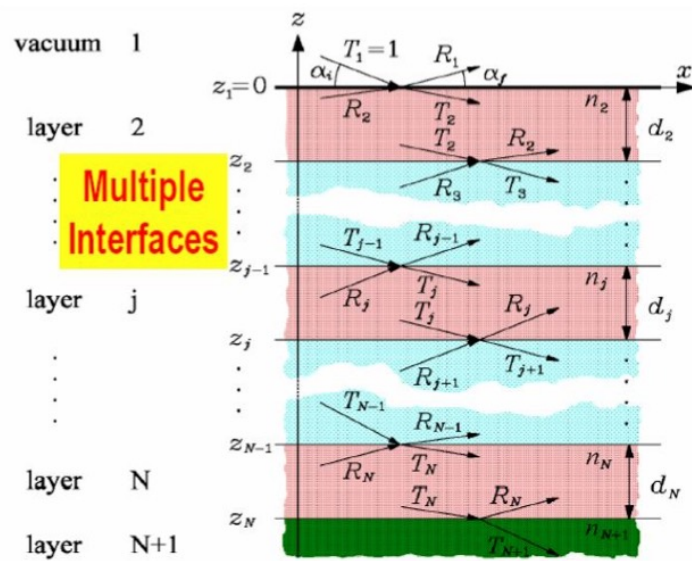


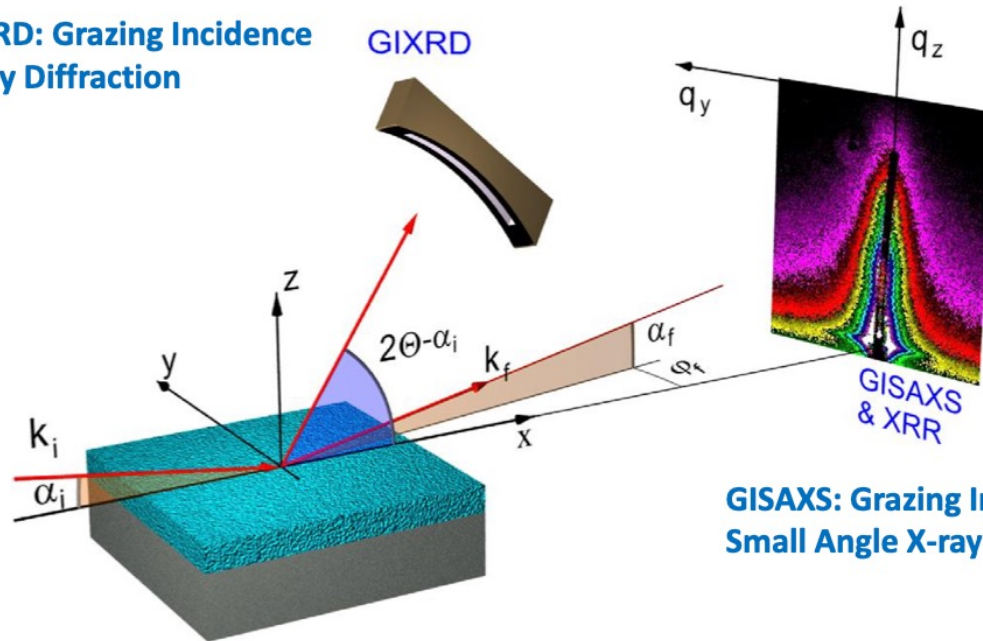
Fig. 8. Information provided by X-ray reflectivity profile.

Reflectivity from Multiple Layers



**GIXRD: Grazing Incidence
X-ray Diffraction**

GIXRD

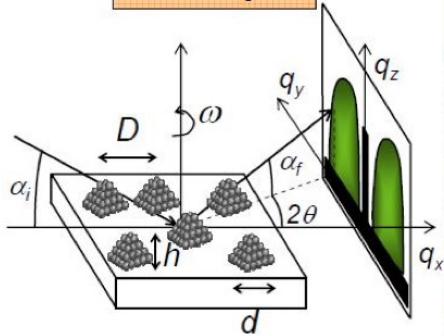


**GISAXS: Grazing Incidence
Small Angle X-ray Scattering**

In GISAXS, the angle α_i is very small ($<0.5^\circ$) for GISAXS, X-ray penetrates the sample and reflection is very strong, beam stopper is required to protect detector.
In our experiment, $\alpha_i = 1.8^\circ$, beam intensity is reduced dramatically, no stopper.

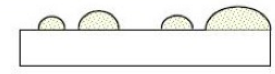
Grazing Incidence Small Angle X-ray Scattering (GISAXS)

Principle

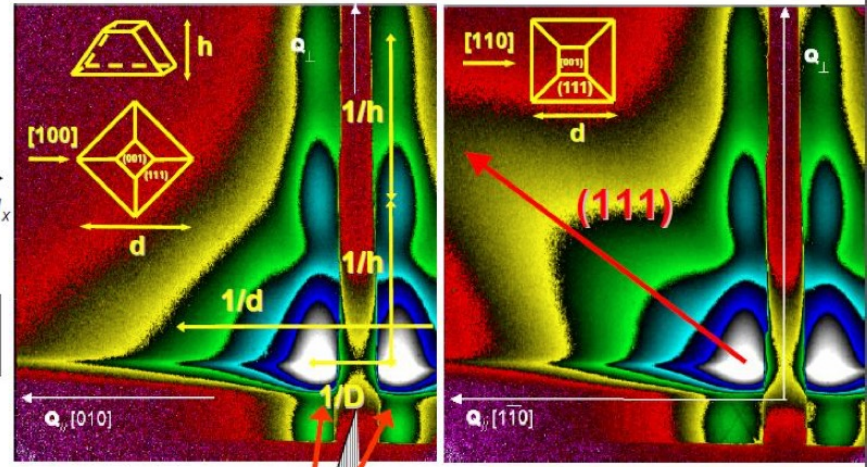


2D image around direct beam:
Fourier transform of objects

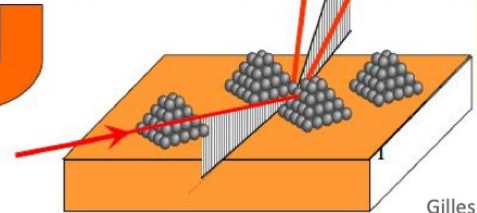
Standard 3D growth (Volmer-Weber)



Example : 20 Å Ag/MgO(001) 500K

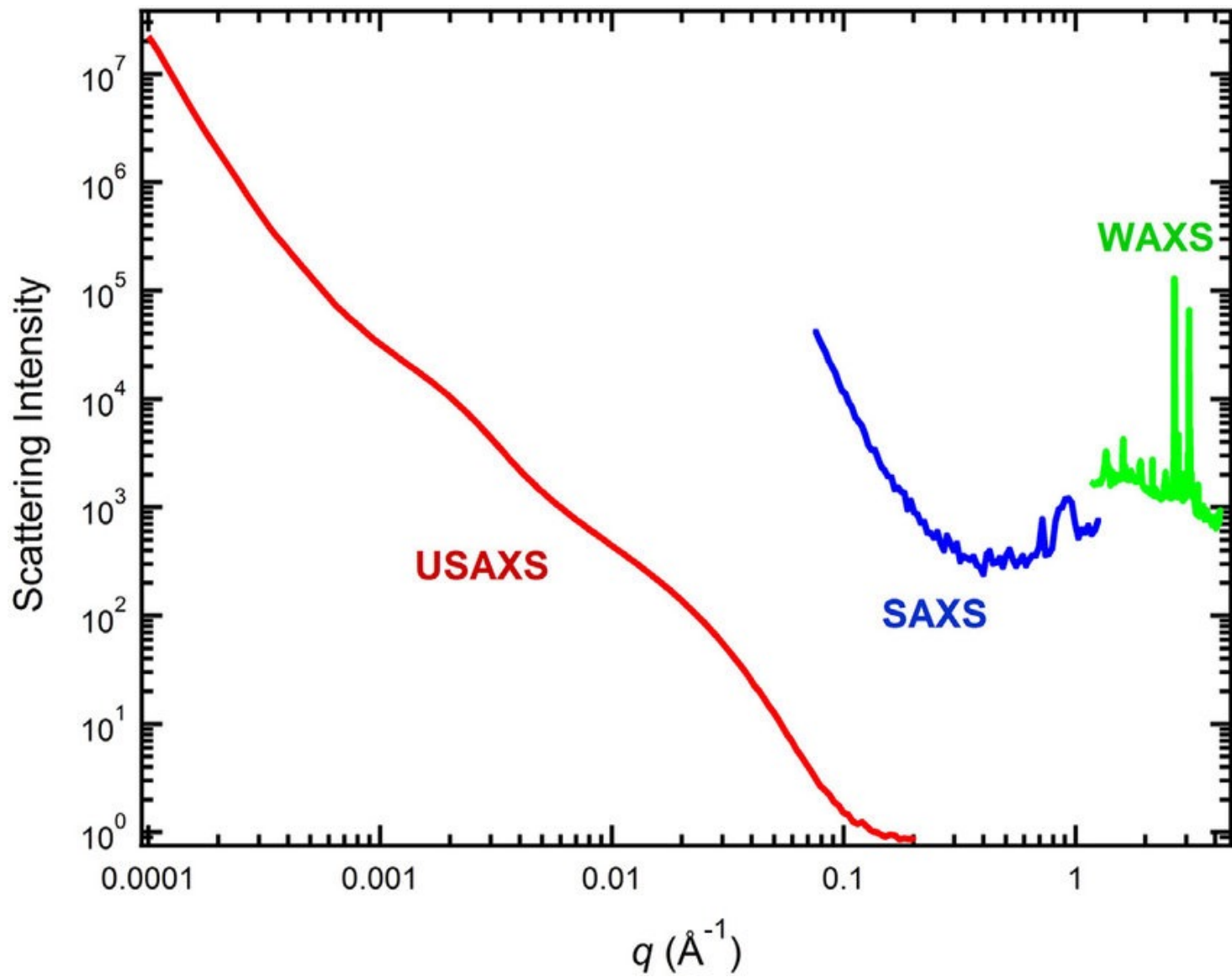


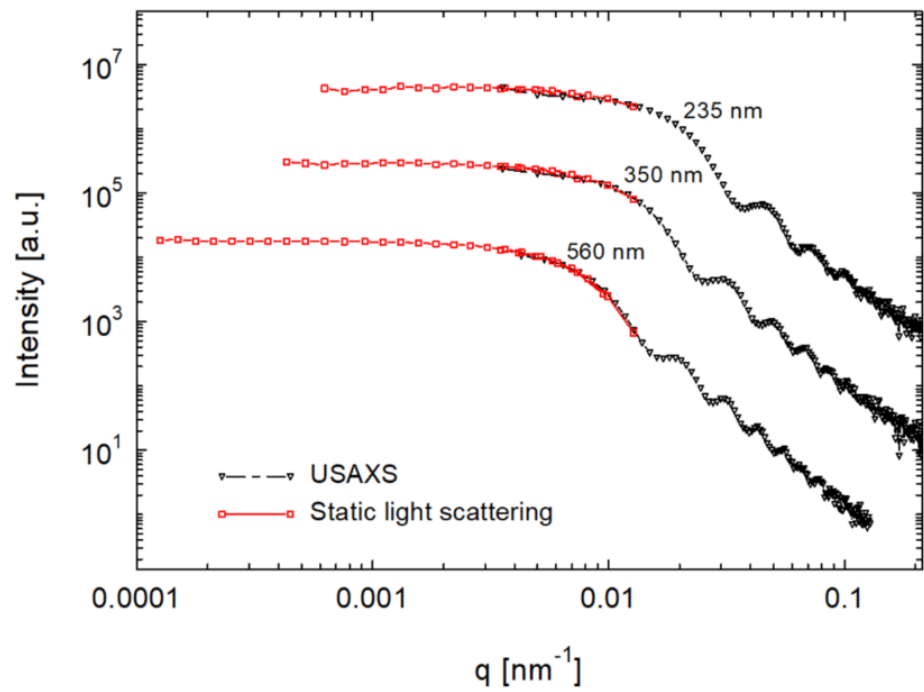
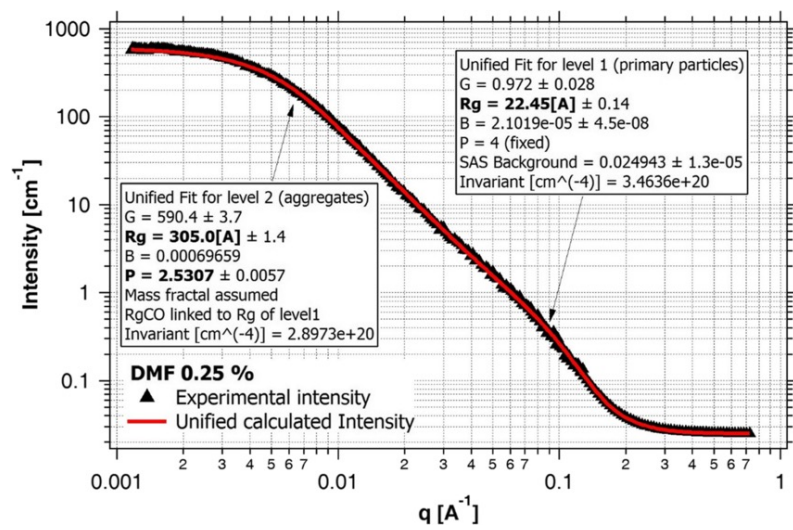
- Morphology
- Shape
 - Sizes
 - Size distributions
 - Particle-particle pair correlation function



Anisotropic islands:
truncated square pyramids
with (111) facets

Gilles Renaud et al. Science 300, 1416 (2003)

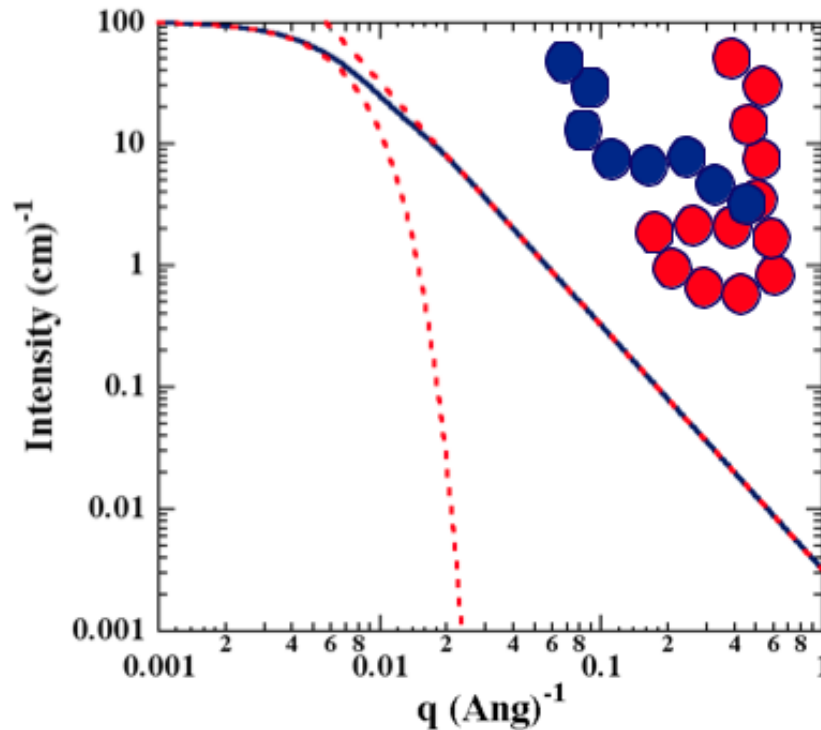




Small-Angle Light, Neutron, and X-ray Scattering for Osmotic Compressibility

“Thermodynamic Limit”

At large sizes contrast arises from thermally driven fluctuations in density that are opposed by the osmotic compressibility, $(d\rho/dP)_T$. The observed intensity $I(q \rightarrow 0) \sim kT / (d\rho/dP)_T$. Here P is Π the osmotic pressure which can be expressed using the virial expansion so that the first derivative is the second virial coefficient A_2 . Low- q scattering can measure the thermodynamic interaction of particles.

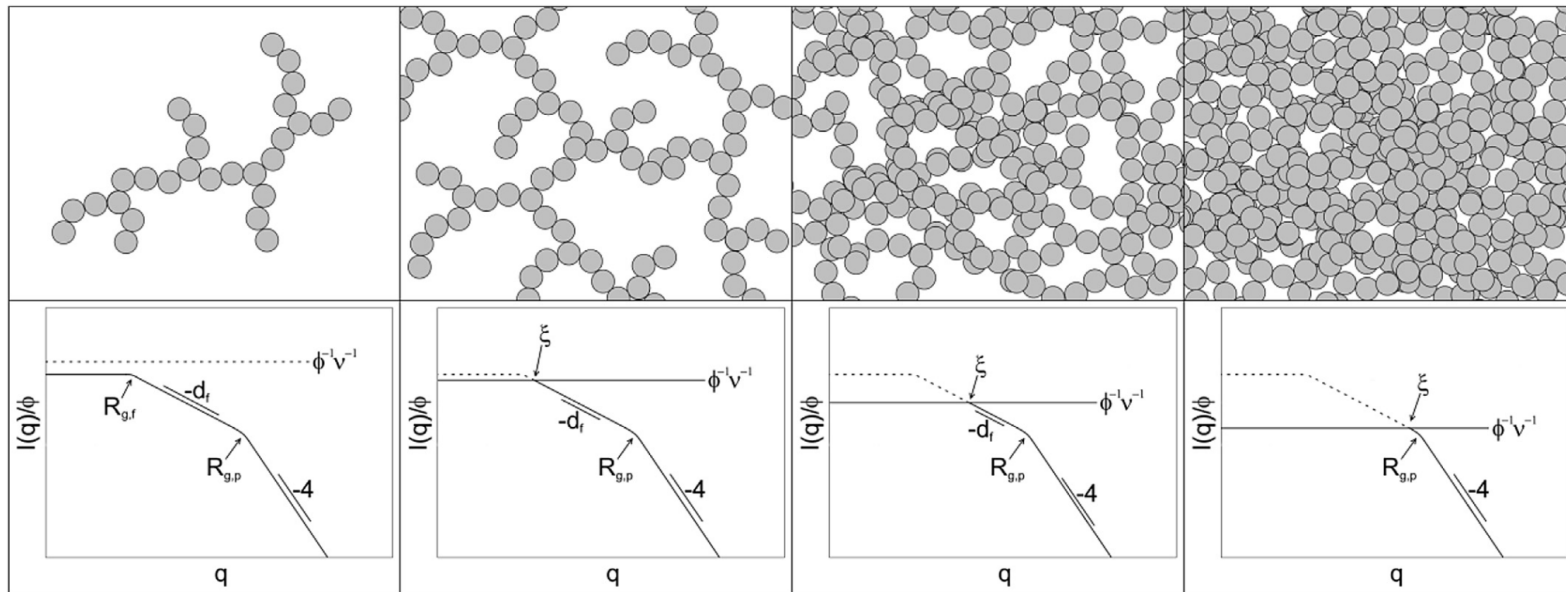


Large size
 $(2\pi/0.001) \text{ \AA} = 600 \text{ nm}$

Small size
 $(2\pi/1) \text{ \AA} = 0.6 \text{ nm}$

$$B_2 = \frac{vM^2\langle\Delta\rho^2\rangle}{2N_a\phi_{filler}^2}$$

Low- q scattering allows measurement of the second virial coefficient B_2



Experimental Thermodynamics (30 common techniques)

Experimental Thermodynamics (30 common techniques)